

# Robust Distance Covariance

Sarah Leyder<sup>1</sup> | Jakob Raymaekers<sup>1</sup> |  
Peter J. Rousseeuw<sup>2</sup>

<sup>1</sup>Department of Mathematics, University of Antwerp, Antwerp, Belgium

<sup>2</sup>Department of Mathematics, University of Leuven, Leuven, Belgium

## Correspondence

Peter J. Rousseeuw, Department of Mathematics, University of Leuven, Celestijnenlaan 220B, BE-3001 Heverlee, Belgium  
Email: peter.rousseeuw@kuleuven.be

## Funding information

The first author was supported by Fonds Wetenschappelijk onderzoek - Vlaanderen (FWO) as a PhD fellow Fundamental Research (PhD fellowship 11K5523N). The second author was supported by the European Union's Horizon 2022 research and innovation program under the Marie Skłodowska Curie grant agreement No 101103017.

Distance covariance is a popular measure of dependence between random variables. It has some robustness properties, but not all. We prove that the influence function of the usual distance covariance is bounded, but that its breakdown value is zero. Moreover, it has an unbounded sensitivity function converging to the bounded influence function for increasing sample size. To address this sensitivity to outliers we construct a more robust version of distance covariance and distance correlation, based on a new data transformation. Simulations indicate that the resulting method is quite robust, and has good power in the presence of outliers. We illustrate the method on genetic data. Comparing the classical distance correlation with its more robust version provides additional insight.

**Keywords** – Breakdown value, Dependence measures, Independence testing, Influence Function, Robust statistics

## 1 | INTRODUCTION

Distance covariance (dCov), proposed by Székely et al. (2007), is a relatively recent measure of dependence between real random variables  $X$  and  $Y$ . Its popularity stems from the fact that  $\text{dCov}(X, Y)$  is zero if and only if  $X$  and  $Y$  are independent, and positive otherwise. Therefore *any* type of dependence makes it nonzero, unlike the product-moment covariance  $\text{Cov}(X, Y)$  which aims specifically for linear relations.

Another feature of dCov is its simple definition. Assume that  $X$  has a finite first moment. Then Székely et al. (2007) compute the *doubly centered* interpoint distances of  $X$ , given by

$$\Delta(X, X') = |X - X'| - E_{X''} [|X - X''|] - E_{X'''} [|X'' - X'|] + E_{X'', X'''} E[|X'' - X'''|] \quad (1)$$

where  $X'$ ,  $X''$  and  $X'''$  are independent copies of  $X$ . Note that  $\Delta(X, X') = \Delta(X', X)$  is not a distance itself, since it also takes on negative values. Moreover,  $E_X[\Delta(X, X')]$  is zero, and the same holds for  $E_{X'}[\Delta(X, X')]$  and  $E_{X, X'}[\Delta(X, X')]$ . This explains the name 'doubly centered'. It turns out that the *second* moments of  $\Delta(X, X')$  exist as well.

If also  $E[|Y|]$  is finite, Székely et al. (2007) introduced the distance covariance defined as

$$\text{dCov}(X, Y) := \text{Cov}(\Delta(X, X'), \Delta(Y, Y')). \quad (2)$$

(In fact they took the square root of the right hand side, but we prefer not to because the units of (2) are those of  $X$  times  $Y$ .) They proved the amazing result that when the first moments of  $X$  and  $Y$  exist, it holds that

$$X \perp\!\!\!\perp Y \iff \text{dCov}(X, Y) = 0. \quad (3)$$

This yields a necessary *and sufficient* condition for independence. The implication  $\Leftarrow$  is not obvious at all, and was proven by complex analysis.

In the same paper also another expression for dCov was derived. Working out the covariance in (2) yields  $4 \times 4 = 16$  terms, that exist when  $X$  and  $Y$  also have second moments. These can be reduced to four and even three terms:

$$\begin{aligned} \text{dCov}(X, Y) &= E[|X - X'| |Y - Y'|] + E[|X - X'|] E[|Y - Y'|] - E[|X - X'| |Y - Y''|] - E[|X - X''| |Y - Y'|] \\ &= E[|X - X'| |Y - Y'|] + E[|X - X'|] E[|Y - Y'|] - 2E[|X - X'| |Y - Y''|]. \end{aligned}$$

In view of the occurrence of terms containing  $X - X'$  and  $Y - Y'$ , Raymaekers and Rousseeuw (2025) investigated various relations between the properties  $X \perp\!\!\!\perp Y$ ,  $(X - X') \perp\!\!\!\perp Y$ , and  $(X - X') \perp\!\!\!\perp (Y - Y')$ .

Based on the distance covariance one also defines the *distance variance* of a variable as

$$\text{dVar}(X) := \text{dCov}(X, X), \quad (4)$$

which has the units of  $X^2$ . The *distance standard deviation* is its square root

$$\text{dStd}(X) := \sqrt{\text{dVar}(X)} \quad (5)$$

with the units of  $X$ . The *distance correlation* is given by

$$\text{dCor}(X, Y) = \frac{\text{dCov}(X, Y)}{\sqrt{\text{dVar}(X) \text{dVar}(Y)}}. \quad (6)$$

The distance correlation has no units and lies between zero and one, and finite sample versions of it are often used to test for independence.

In this paper  $X$  and  $Y$  will typically be univariate random variables, but the above definitions can also be used for multivariate variables, in which case  $|\cdot|$  stands for the Euclidean norm. Székely and Rizzo (2012) generalized these notions to  $\alpha$ -distance dependence measures where  $0 < \alpha < 2$ . If the moments of order  $2\alpha$  of  $|X|$  and  $|Y|$  are finite,

$d\text{Cov}(X, Y; \alpha)$  is defined as

$$d\text{Cov}(X, Y; \alpha) = \mathbb{E}[|X - X'|^\alpha |Y - Y'|^\alpha] + \mathbb{E}[|X - X'|^\alpha] \mathbb{E}[|Y - Y'|^\alpha] - 2\mathbb{E}[|X - X'|^\alpha |Y - Y''|^\alpha]$$

for i.i.d.  $(X, Y)$ ,  $(X', Y')$ , and  $(X'', Y'')$ . It satisfies the equivariance property

$$d\text{Cov}(a_1 + b_1 X, a_2 + b_2 Y; \alpha)^{1/\alpha} = b_1 b_2 d\text{Cov}(X, Y; \alpha)^{1/\alpha}$$

for all  $a_1, a_2, b_1 > 0$ , and  $b_2 > 0$ . For appropriate measurement units we should thus work with  $d\text{Cov}(\cdot, \cdot, \alpha)^{1/\alpha}$  when  $\alpha \neq 1$ .

Distance covariance is a general method with interesting properties and wide ranging applications, for instance in feature selection (Song et al., 2012), sparse contingency tables (Zhang, 2019), and time series (Zhou, 2012; Davis et al., 2018). Fast algorithms for its computation have been constructed (Huo and Székely, 2016; Chaudhuri and Hu, 2019). Sejdinovic et al. (2013) and Edelman and Goeman (2022) found interesting connections with other dependence measures, such as the Hilbert-Schmidt Independence Criterion of Gretton et al. (2005).

The distance covariance and distance correlation have sometimes been credited with natural robustness properties, see e.g. Matteson and Tsay (2017), Chen et al. (2018), Kasieczka and Shih (2020) and Ugwu et al. (2023), but to the best of our knowledge they have not yet been formally investigated from this perspective.

In Sections 2 and 3 we study the robustness of  $d\text{Cov}$  and  $d\text{Var}$  against outliers by deriving influence functions and breakdown values. Section 4 then constructs a new approach to make  $d\text{Cov}$  and  $d\text{Cor}$  more robust. The new method is compared with alternatives in Section 5, and it is illustrated on a real data example in Section 6. Section 7 provides an outlook on potential applications, and Section 8 concludes.

## 2 | INFLUENCE FUNCTIONS

Let  $T$  be a statistical functional that maps a bivariate distribution  $F$  to a scalar. Following Hampel et al. (1986), the *influence function* (IF) of  $T$  at  $F$  is defined as

$$\text{IF}((s, t), T, F) = \lim_{\varepsilon \rightarrow 0} \frac{T((1 - \varepsilon)F + \varepsilon\Delta_{(s,t)}) - T(F)}{\varepsilon} = \left. \frac{\partial}{\partial \varepsilon} T((1 - \varepsilon)F_\rho + \varepsilon\Delta_{(s,t)}) \right|_{\varepsilon=0+} \quad (7)$$

for any  $(s, t)$ , where  $\Delta_{(s,t)}$  is the probability distribution that puts all its mass in the point  $(s, t)$ . The IF quantifies the effect of a small amount of contamination in  $(s, t)$  on  $T$ . The supremum of the influence function  $\gamma^*(T) := \sup_{(s,t) \in \mathbb{R}^2} |\text{IF}((s, t), T, F)|$  is called the *gross-error sensitivity*. One goal of robust estimation is to have a finite gross-error sensitivity, or equivalently, to have a bounded influence function.

Let  $(X, Y)$  be a bivariate random vector with distribution  $F$ , with marginal distributions  $F_X$  and  $F_Y$ . We can then consider the distance covariance and distance correlation as statistical functionals that map  $F$  to the population value of their respective quantities. In this section we will derive the influence functions of the distance covariance and the distance correlation, and study their behavior.

### 2.1 | Distance covariance

The influence function of the  $\alpha$ -distance covariance is given in the following result:

**Proposition 1** Assume  $E[|X|^{2\alpha}] < \infty$  and  $E[|Y|^{2\alpha}] < \infty$ . The influence function of the  $\alpha$ -distance covariance between  $X$  and  $Y$  is given by

$$IF((s, t), dCov(X, Y; \alpha), F) = -2dCov(X, Y; \alpha) + 2\eta(s, t, X, Y, \alpha),$$

where

$$\eta(s, t, X, Y, \alpha) := Cov(|X - s|^\alpha - |X - X'|^\alpha, |Y - t|^\alpha - |Y - Y''|^\alpha).$$

We have introduced the notation  $\eta(s, t, X, Y, \alpha)$  for the second term of the IF. This is the quantity that depends on the position of the contamination  $(s, t)$ , and it governs the behavior of most influence functions that we will consider. The derivations of all our influence function results can be found in Section A of the Supplementary Material.

Figure 1 shows the IF of the distance covariance for various values of  $\alpha$ , when  $(X, Y)$  follows a bivariate normal distribution with mean zero, unit variances, and correlation  $\rho = 0.6$ . The contamination is placed at  $(s, t) = (s, s)$  in the left panel, and at  $(s, t) = (s, -s)$  in the right panel. We compare the influence functions of  $c_\alpha dCov(\cdot, \cdot; \alpha)^{1/\alpha}$  where  $c_\alpha := dCov(X, Y; 1)/dCov(X, Y; \alpha)^{1/\alpha}$ . The exponent  $1/\alpha$  gives the quantities under comparison the same units. Moreover, the factor  $c_\alpha$  ensures that all measures estimate the same population quantity on uncontaminated data. Without these adjustments, the influence functions would not be directly comparable.

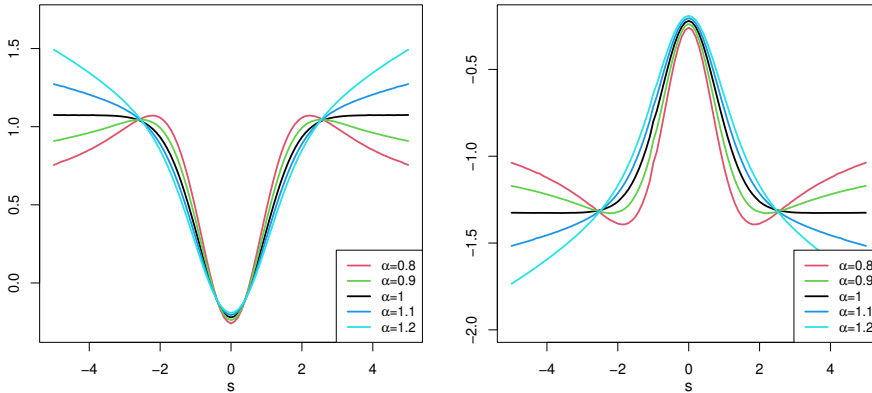


**FIGURE 1** Influence function of  $c_\alpha dCov(\cdot, \cdot; \alpha)^{1/\alpha}$  for different values of  $\alpha$ . The left panel shows the IF in  $(s, t) = (s, s)$ , whereas right panel shows it in  $(s, t) = (s, -s)$ . Here  $(X, Y)$  follows a bivariate normal distribution with correlation  $\rho = 0.6$ .

For small and intermediate values of  $s$ , the influence functions are roughly quadratic in  $|s|$  and behave very similarly. However, the behavior for large values of  $|s|$  depends strongly on  $\alpha$ . We see that for  $\alpha < 1$  the IF is not only bounded but re-descends towards zero. For  $\alpha > 1$  the IF becomes unbounded. This is not unexpected because  $c_\alpha dCov(\cdot, \cdot; \alpha)^{1/\alpha}$  becomes proportional to the absolute value of the classical covariance between  $X$  and  $Y$  when  $\alpha \rightarrow 2$ . The standard choice  $\alpha = 1$  plays a special role, as the highest value of  $\alpha$  for which the IF is bounded. We formalize this behavior in the proposition below.

**Proposition 2** The IF of the  $\alpha$ -distance covariance has the following properties:

- If  $\alpha > 1$  then  $IF((s, t), dCov(X, Y; \alpha), F)$  can be unbounded.

- If  $\alpha = 1$  then  $IF((s, t), dCov(X, Y; \alpha), F)$  is bounded.
- If  $\alpha < 1$  then  $IF((s, t), dCov(X, Y; \alpha), F)$  is bounded and redescending.

The dependency structure between  $X$  and  $Y$  affects the behavior for  $\alpha > 1$ . If  $X$  and  $Y$  are independent, then  $\eta(s, t, X, Y, \alpha) = 0$  so the IF remains bounded. At the other extreme, if  $X = Y$  they are perfectly dependent, and  $IF((s, s), dCov(X, Y; \alpha), F) = IF(s, dVar(X; \alpha), F_X)$  is unbounded for  $\alpha > 1$  as we will see in the next section.

## 2.2 | Distance variance and standard deviation

From the IF of the distance covariance we can derive those of  $dVar$  and  $dStd$ .

**Corollary 1** *The influence functions of  $dVar$  and  $dStd$  are given by*

$$IF(s, dVar(X; \alpha), F) = -2dVar(X; \alpha) + 2\eta(s, s, X, X, \alpha)$$

$$IF(s, dStd(X; \alpha), F) = \frac{-2dVar(X; \alpha) + 2\eta(s, s, X, X, \alpha)}{2dStd(X; \alpha)}$$

The left panel of Figure 2 plots the IF of the quantities  $v_\alpha dVar(\cdot; \alpha)^{1/\alpha}$  with  $v_\alpha := dVar(X; 1)/dVar(X; \alpha)^{1/\alpha}$  that are comparable across  $\alpha$ . Here  $F$  is the standard normal distribution. The behavior of the IF again depends on  $\alpha$ . In particular,  $\alpha = 1$  is the highest value for which the IF is bounded. Larger  $\alpha$  yield unbounded influence functions, whereas smaller  $\alpha$  lead to redescending curves.

**Proposition 3** *The IF of the  $\alpha$ -distance variance has the following properties:*

- If  $\alpha > 1$  then  $IF(s, dVar(X; \alpha), F)$  is unbounded.
- If  $\alpha = 1$  then  $IF(s, dVar(X; \alpha), F)$  is bounded.
- If  $\alpha < 1$  then  $IF(s, dVar(X; \alpha), F)$  is bounded and redescending.

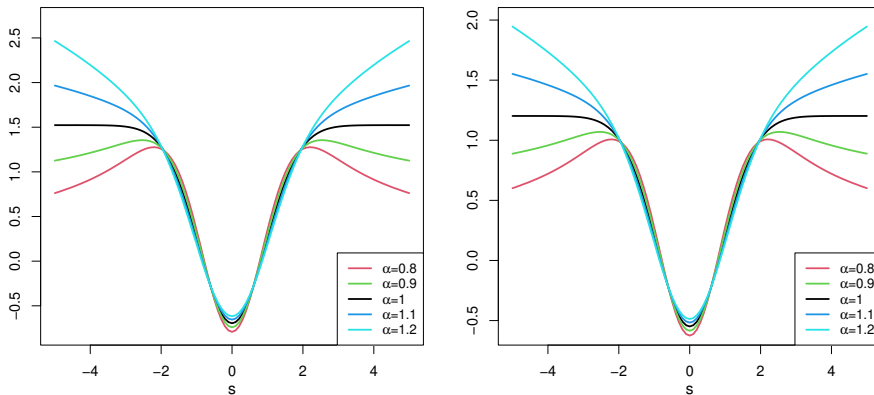


**FIGURE 2** Influence function of  $v_\alpha dVar(\cdot; \alpha)^{1/\alpha}$  (left) and  $v_\alpha^{1/2} dStd(\cdot; \alpha)^{1/\alpha}$  (right) for different values of  $\alpha$ , for standard normal data.

As  $dVar$  and  $dStd$  are scale estimators, we can compare them with popular alternatives. We need to be careful though,

since different scale estimators may be estimating different population quantities. For instance, if we want to estimate the variance of a Gaussian distribution we need a consistency factor for  $d\text{Var}$ . For  $\alpha = 1$ , Székely et al. (2007) find at the standard normal distribution that

$$d\text{Var}(X) = d\text{Cov}(X, X) = \frac{4}{3\pi} (\pi - 3\sqrt{3} + 3).$$

For  $X \sim \mathcal{N}(0, \sigma^2)$  and  $c := 3\pi/(4(\pi - 3\sqrt{3} + 3))$  we thus obtain  $c d\text{Var}(X) = \sigma^2$  and  $\sqrt{c} d\text{Std}(X) = \sigma$ . For other  $\alpha$  we use  $v_\alpha c d\text{Var}^{1/\alpha}(X)$  with  $v_\alpha := d\text{Var}(X; 1)/d\text{Var}(X; \alpha)^{1/\alpha}$ .

Figure 3 plots the influence function of  $d\text{Std}(X; \alpha)^{1/\alpha}$  with its consistency factor. It also contains the IF of the classical standard deviation  $\text{Std}$ , and the MAD given by  $1.483 \text{median}(X - \text{median}(X))$ . We know  $d\text{Std}(X; \alpha)^{1/\alpha}$  becomes proportional to  $\text{Std}$  for  $\alpha \rightarrow 2$ , which explains why its influence function tends to a parabola.

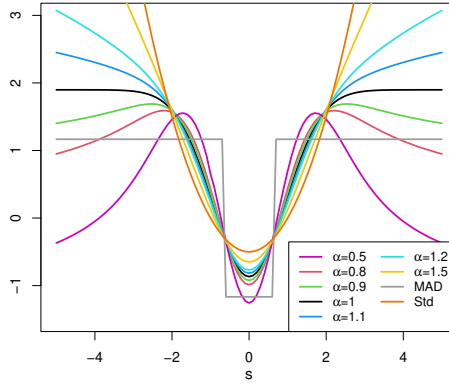


**FIGURE 3** Influence function of different scale estimators, including  $\sqrt{v_\alpha c} d\text{Std}(X; \alpha)^{1/\alpha}$  for various  $\alpha$ , the MAD, and the classical standard deviation  $\text{Std}$ .

A further investigation of the  $\alpha$ -distance standard deviation as a scale estimator can be found in Section B of the Supplementary Material.

### 2.3 | Distance correlation

Based on Proposition 1 and Corollary 1 we now obtain the IF of the distance correlation.

**Corollary 2** The influence function of  $d\text{Cor}$  is given by

$$IF((s, t), d\text{Cor}(X, Y; \alpha), F) = \frac{2\eta(s, t, X, Y, \alpha)}{d\text{Std}(X; \alpha) d\text{Std}(Y; \alpha)} - d\text{Cor}(X, Y; \alpha) \left( \frac{\eta(s, s, X, X, \alpha)}{d\text{Var}(X; \alpha)} + \frac{\eta(t, t, Y, Y, \alpha)}{d\text{Var}(Y; \alpha)} \right).$$

Figure 4 shows the IF of  $r_\alpha d\text{Cor}(\cdot, \cdot; \alpha)^{1/\alpha}$  on bivariate normal data with correlation  $\rho = 0.6$ , with  $r_\alpha := d\text{Cor}(\cdot, \cdot; 1)/d\text{Cor}(\cdot, \cdot; \alpha)^{1/\alpha}$ . The behavior of the IF is similar to that in Figure 1.

**Proposition 4** The influence function of the  $\alpha$ -distance correlation satisfies:

- If  $\alpha > 1$  then  $IF((s, t), d\text{Cor}(X, Y; \alpha), F)$  can be unbounded.

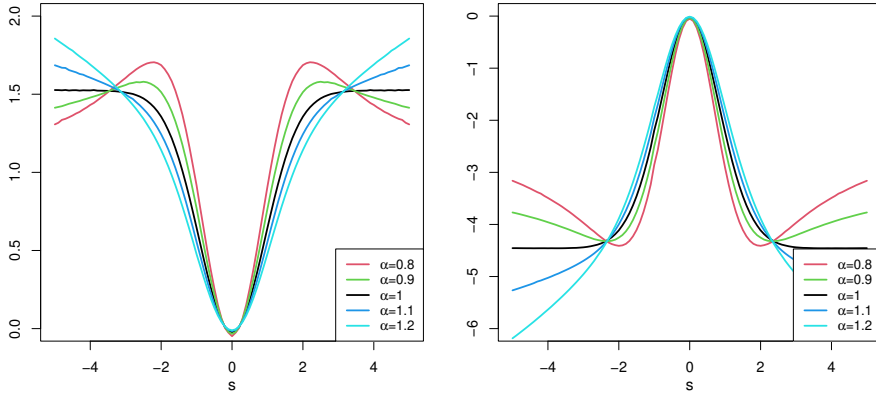


**FIGURE 4** Influence function of  $r_\alpha \text{dCor}(\cdot, \cdot; \alpha)^{1/\alpha}$  for various  $\alpha$ . The left panel shows  $(s, t) = (s, s)$ , whereas the right panel shows  $(s, t) = (s, -s)$ . Here  $(X, Y)$  follows a bivariate normal distribution with  $\rho = 0.6$ .

- If  $\alpha = 1$  then  $IF((s, t), \text{dCor}(X, Y; \alpha), F)$  is bounded.
- If  $\alpha < 1$  then  $IF((s, t), \text{dCor}(X, Y; \alpha), F)$  is bounded and re-descending.

### 3 | BREAKDOWN VALUES

From the study of the influence functions in Section 2 one may conclude that  $\text{dCov}$  and  $\text{dCor}$  indeed have natural robustness properties when  $\alpha \leq 1$ , and even a re-descending nature when  $\alpha < 1$ . However, the IF only tells part of the story. Here we complement the analysis with a discussion of the breakdown value, a popular and intuitive measure of robustness. It quantifies how much contamination an estimator can take before it becomes completely uninformative, i.e., it carries no information about the uncontaminated data.

The *finite-sample breakdown value* (Donoho and Huber, 1983) of an estimator  $T$  at a dataset  $Z$  is the smallest fraction of observations that needs to be replaced to make the estimate useless. Here  $Z$  is a dataset of size  $n$ , and we denote by  $Z^m$  any corrupted dataset obtained by replacing at most  $m$  cases of  $Z$  by arbitrary cases. Then the finite-sample breakdown value of  $T$  at  $Z$  is defined as

$$\varepsilon_n^*(T, Z) = \min \left\{ \frac{m}{n} : \sup_{Z^m} |T(Z^m) - T(Z)| = \infty \right\}.$$

We now investigate the finite-sample breakdown value of the distance variance. For a univariate sample  $X_n$  we denote  $d_{ij} := |x_i - x_j|^\alpha$  for  $\alpha > 0$ . (In higher dimensions  $|\cdot|$  would be interpreted as the Euclidean norm.) Double centering yields the values

$$\Delta_{ij} := d_{ij} - \bar{d}_{i.} - \bar{d}_{.j} + \bar{d}_{..}$$

so  $\sum_{j=1}^n \Delta_{ij} = 0$  for all  $i$  and  $\sum_{i=1}^n \Delta_{ij} = 0$  for all  $j$ .

Now we replace the observation  $x_1$  by a large number  $s > 0$  that we will let go to infinity afterward. [For  $s < 0$  we would write  $|s|$  below, and in higher dimensions we could replace  $x_1$  by e.g.  $(s, 0, \dots, 0)$ .] When  $s$  grows, the  $n - 1$

values  $d_{1j} = |s - x_j|^\alpha$  for  $j \neq 1$  are of the order  $s^\alpha$ . We can think of the  $x_j$  as small relative to  $s$ , and positioned around zero. We will write the quantities of interest in terms of the variable  $u := s^{\alpha/2}$ . This yields

$$d_{1j} = |s - x_j|^\alpha = ((s - x_j)^2)^{\alpha/2} = u^2 + O(u).$$

From this we derive expressions for  $\overline{d_i}, \overline{d_j}, \overline{d_{..}}$ , as well as  $\Delta_{ij}$  in Section C.1 of the Supplementary Material. Combining these, the distance variance of  $X_n$  becomes

$$\text{dVar}(X_n; \alpha) = 4 \frac{(n-1)^2}{n^4} u^4 + O(u^3).$$

For large  $s$  and sample size  $n$  we thus obtain

$$\text{dVar}(X_n; \alpha) \approx \frac{4}{n^2} s^{2\alpha} + O(s^{3\alpha/2}) \quad (8)$$

which goes to infinity with  $s$  (for any  $\alpha > 0$ ), so the breakdown value of  $\text{dVar}$  is only  $\frac{1}{n} \approx 0$ . This says that a single outlier can destroy it.

Interestingly, this does not contradict the fact that the influence function is bounded for  $\alpha \leq 1$ . This is because the denominator of the leading term of the right hand side of (8) contains  $n^2$  instead of the usual  $n$ . To see the effect of this, note that the contamination mass  $\varepsilon$  in the definition of the influence function corresponds to  $\frac{1}{n}$ , hence

$$\begin{aligned} \text{IF}(s, \text{dVar}, F) &= \frac{\partial}{\partial \varepsilon} [\text{dVar}(F_\varepsilon)]_{\varepsilon=0} = \lim_{\varepsilon \rightarrow 0^+} \frac{\text{dVar}(F_\varepsilon) - \text{dVar}(F)}{\varepsilon} \\ &= \lim_{\varepsilon \rightarrow 0^+} \frac{4\varepsilon^2 s^{2\alpha}}{\varepsilon} + \lim_{\varepsilon \rightarrow 0^+} \frac{O(s^{3\alpha/2})}{\varepsilon} = \lim_{\varepsilon \rightarrow 0^+} 4\varepsilon s^{2\alpha} + \lim_{\varepsilon \rightarrow 0^+} \frac{O(s^{3\alpha/2})}{\varepsilon} \end{aligned}$$

so the highest order term in  $s$  vanishes due to the remaining factor  $\varepsilon$ , whereas the next term corresponds to the IF.

This might be the first occurrence of a natural statistic with a bounded IF and a zero breakdown value. The opposite situation was known before, for instance the normal scores R-estimator of location has an unbounded IF and a positive breakdown value of 23.9%, see page 112 of Hampel et al. (1986). Also, the normal scores correlation coefficient has unbounded IF and breakdown value 12.4% (Boudt et al., 2012). But a combination of a bounded IF with a zero breakdown value appears to be new. In retrospect we can construct artificial but simpler estimators with these properties, such as a modified trimmed mean. The usual 10% trimmed mean is given by

$$T(X_n) = \frac{\sum_{i=1}^n w_i x_{i:n}}{\sum_{i=1}^n w_i}$$

where  $x_{1:n} \leq \dots \leq x_{n:n}$  and the  $w_i$  are 1, except for the first and last 10% of them for which  $w_i = 0$ . If we instead put the first and last 10% of them equal to  $w_i = 1/n^2$  then the breakdown value will go down from 10% to  $1/n \approx 0$ , but the influence function will remain the same as that of the usual 10% trimmed mean.

The *sensitivity curve* of an estimator  $T$  is a finite-sample version of the IF, given by

$$\text{SC}(s, T, (x_1, \dots, x_n)) := n (T(s, x_1, \dots, x_n) - T(x_1, \dots, x_n)) \quad (9)$$

at a dataset  $(x_1, \dots, x_n)$ . Here we set  $x_i = \Phi^{-1}((i - \frac{1}{2})/(n + \frac{1}{2}))$  for illustration purposes. Note that (8) implies that

the sensitivity curve of the distance variance for  $\alpha = 1$  is unbounded, since it becomes arbitrarily high for large  $s$ . This also seems to be at odds with the fact that the IF is bounded. However, the unbounded sensitivity curve does converge to the bounded IF for increasing sample size  $n$ . This is illustrated in Figure 5 which shows the sensitivity curve for a wide range of  $s$ , for different sample sizes  $n$ .

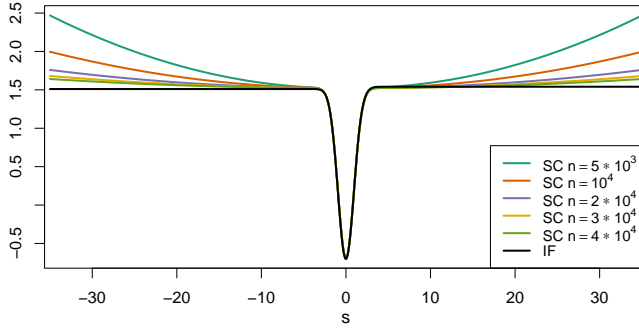


**FIGURE 5** Unbounded sensitivity curve of dVar for different sample sizes  $n$ , which converges for  $n \rightarrow \infty$  to the bounded influence function.

For the breakdown of dCov we start from a bivariate dataset  $Z = [X_n; Y_n] = \{(x_i, y_i); i = 1, \dots, n\}$  and replace  $(x_1, y_1)$  by some  $(s, t)$  for large positive  $s$  and  $t$ . In Section C.1 of the Supplementary Material we then obtain

$$\text{dCov}(X_n, Y_n; \alpha) \approx \frac{4}{n^2} s^\alpha t^\alpha + O(s^{3\alpha/4} t^{3\alpha/4}), \quad (10)$$

so the breakdown value of dCov is  $\frac{1}{n} \rightarrow 0$  as well.

Note that (10) implies that the sensitivity surface of the distance covariance is unbounded, since it grows without bound for large arguments  $s$  and  $t$ . But when  $\alpha \leq 1$  the unbounded sensitivity surface does converge to the bounded influence function for increasing sample size  $n$ . The situation is analogous to the illustration in Figure 5.

For dCor we can for instance take  $t = s$ . Then we obtain

$$\text{dCor}(X_n, Y_n) = \frac{\text{dCov}(X_n, Y_n)}{\sqrt{\text{dVar}(X_n)} \sqrt{\text{dVar}(Y_n)}} \rightarrow 1 \quad (11)$$

for  $s \rightarrow \infty$ . So replacing a single data point can bring dCor arbitrarily close to 1, even if the variables  $X$  and  $Y$  are independent. This can also be seen as breakdown.

So far we have looked at the finite-sample breakdown value, but we can also compute the asymptotic version. For the distance variance we consider the distribution  $F$  of  $X$ . We can construct contaminated distributions  $F_\varepsilon = (1 - \varepsilon)F + \varepsilon H$  where  $H$  may be any distribution. The asymptotic breakdown value is then defined as

$$\varepsilon^*(\text{dVar}) = \inf\{\varepsilon; \sup_H \text{dVar}((1 - \varepsilon)F + \varepsilon H) = \infty\}.$$

Section C.2 of the Supplementary Material shows that  $\varepsilon^*(\text{dVar}) = 0$  by inserting distributions  $H = \Delta_s$  for  $|s| \rightarrow \infty$ .

For the asymptotic breakdown value of dCov we contaminate the bivariate distribution  $F$  of  $(X, Y)$ , and define

$$\varepsilon^*(\text{dCov}) = \inf\{\varepsilon; \sup_H \text{dCov}((1 - \varepsilon)F + \varepsilon H) = \infty\}.$$

Section C.3 of the Supplementary Material shows that  $\varepsilon^*(\text{dCov}) = 0$  by employing  $H = \Delta_{(s,s)}$  for  $|s| \rightarrow \infty$ . One can verify that (11) also holds in the asymptotic setting.

Whether finite-sample or asymptotic, the only way to prevent breakdown of dCov and dCor is to ensure that  $s$  and  $t$  remain bounded.

## 4 | ROBUSTNESS BY TRANSFORMATION

From the results of Sections 2 and 3, it is clear that if we want a strictly positive breakdown value we cannot use dCov directly, no matter the value of  $\alpha$ . One could think of applying a robust covariance measure to the doubly centered distances, but that may lose the crucial property that a population result of zero implies  $X \perp\!\!\!\perp Y$ .

However, if we first apply a bounded transformation to  $X$  and  $Y$  prior to computing dCov and dCor, the breakdown value would be strictly larger than 0 and the influence function would be bounded for any  $\alpha$ . We will consider dependence measures of the type

$$\text{dCor}(\psi_1(X), \psi_2(Y); 1) \tag{12}$$

where the  $\psi_j$  are bounded functions transforming  $X$  and  $Y$ . The  $\psi_j$  have to be invertible, so that independence of  $\psi_1(X)$  and  $\psi_2(Y)$  implies independence of  $\psi_1^{-1}(\psi_1(X)) = X$  and  $\psi_2^{-1}(\psi_2(Y)) = Y$ . Some suggestions in this direction have been made before. For instance, Székely and Rizzo (2023) suggest computing the distance correlation after transforming the data to ranks, which corresponds to using  $\psi_1(x) = F_X(x)$  and  $\psi_2(y) = F_Y(y)$ , the cumulative distribution functions of  $X$  and  $Y$ . Mai et al. (2023) apply dCor after transforming  $X$  and  $Y$  to normal scores (also called Gaussian ranks), by the unbounded transformation  $\psi_j(t) = \Phi^{-1}(F_j(t))$  with  $\Phi$  the standard Gaussian cdf. This approach of computing a classical estimator after marginal transformation of the variables has also been used successfully in the context of correlation estimation in high dimensions (Raymaekers and Rousseeuw, 2021). In that study, transformations with a continuous  $\psi$  that is redescending in the sense that  $\lim_{x \rightarrow \pm\infty} |\psi(x)| = 0$  turned out to be most effective, in line with the success of such  $\psi$ -functions for M-estimation of location in Andrews et al. (1972).

This raises a question: is it possible to design a bounded transformation  $\psi$  which (i) is invertible so we keep the independence property, and (ii) is continuous and redescending? At first sight this seems impossible: any invertible continuous function  $\psi : \mathbb{R} \mapsto \mathbb{R}$  has to be strictly monotone, so it cannot be redescending. However, if the goal is to quantify (in)dependence of random variables, we need not stay in one dimension, and can in fact allow the image of  $\psi$  to be in  $\mathbb{R}^2$ . This unlocks the possibility of creating a  $\psi$ -function which is simultaneously continuous, invertible, and redescending. We propose to use the function  $\psi_\infty : \mathbb{R} \rightarrow \mathbb{R}^2 : x \mapsto (u(x), v(x))$  with

$$u(x) = \begin{cases} c(1 + \cos(2\pi \tanh(x/c) + \pi)) & \text{if } x \geq 0 \\ -c(1 + \cos(2\pi \tanh(x/c) - \pi)) & \text{if } x < 0 \end{cases}$$

$$v(x) = \sin(2\pi \tanh(x/c))$$

where  $c > 0$  is a tuning constant with default  $c = 4$  that gave good results in simulations. We apply this function to

robustly standardized data variables, that is, their median is set to 0 and their MAD to 1. Note that the image of  $\psi_\infty$  is a combination of two ellipses around  $(c, 0)$  and  $(-c, 0)$ , since  $\psi_\infty(\mathbb{R}) = \{(u, v) \in \mathbb{R}^2; \|(u - c, cv)\| = c \text{ or } \|(u + c, cv)\| = c\}$ . Figure 6 illustrates the function  $\psi_\infty$ . As the argument increases from  $x = 0$ ,  $\psi_\infty(x)$  first moves to the right away from the origin, but for  $x/c > 4 \tanh^{-1}(\frac{1}{2}) \approx 2.2$  it returns on the ellipse, and  $\lim_{x \rightarrow \pm\infty} |\psi_\infty(x)| = 0$ . We call  $\psi_\infty$  a *biloop function*. Here ‘loop’ refers to an ellipse, and ‘bi’ alludes to the number of ellipses, the bivariate nature of  $\psi_\infty$ , and the redescending nature of the biweight function (Beaton and Tukey, 1974).

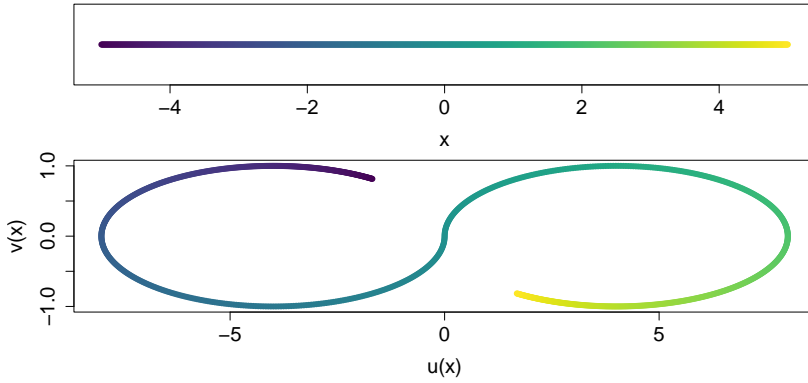


**FIGURE 6** Illustration of the biloop transformation.

We now consider the biloop dCor, i.e., the distance correlation after the  $\psi_\infty$  transformation, as in (12). Due to the bounded and redescending nature of the biloop transformation, the biloop dCor has a bounded and redescending influence function. Figure 7 shows this influence function and compares it to the influence functions of the classical dCor with  $\alpha = 1$ , as well as to the dCor after rank transform (Székely and Rizzo, 2023) and after normal scores (Mai et al., 2023). For the expressions of these influence functions we refer to Section D of the Supplementary Material.

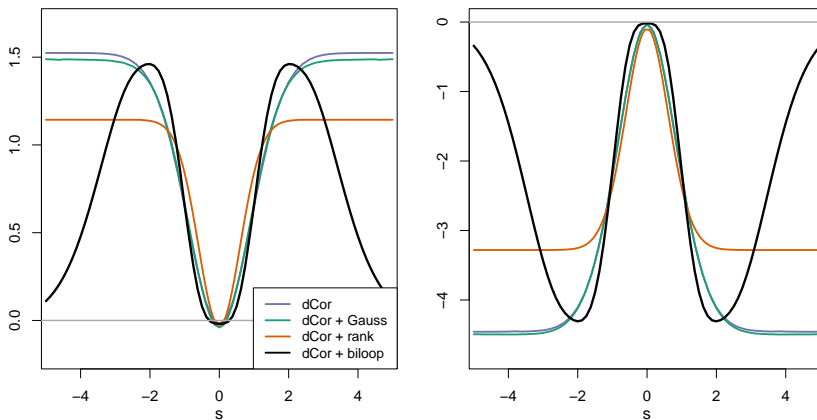


**FIGURE 7** IF of  $dCor(\psi(X), \psi(Y); 1)$  where  $\psi$  is the identity, the normal score (Gaussian rank), the rank transform, or the biloop. The left panel shows  $(s, t) = (s, s)$ , whereas the right panel shows  $(s, t) = (s, -s)$ . Here  $(X, Y)$  is bivariate normal with correlation  $\rho = 0.6$ .

We see that the biloop dCor indeed has a redescending influence function. Using the rank transform does lead to a lower gross-error sensitivity, but does not yield a redescending influence function. The difference between the classical dCor and dCor after normal scores is tiny. This similarity is to be expected since the model distribution in this plot is Gaussian too.

We end with a remark on the utility of a highly robust measure of independence. The robustness properties of the biloop dCor make it less sensitive to observations in the tails of the distribution, far away from the center. In contrast, the classical dCor picks up dependence in these tails very easily. In some situations we may want to focus on dependence in the tails, and in other situations we may prefer not to. In general, comparing the classical dCor with the robust version helps to identify whether the dependence was mainly in the tails or rather in the center of the data.

## 5 | EMPIRICAL RESULTS

### 5.1 | Power simulation

In this simulation we study the power of dCor after applying the transformations discussed in Section 4. More precisely, we compare the original  $dCor(X, Y)$  with the proposed biloop dCor given by  $dCor(\psi_\infty(X), \psi_\infty(Y))$ , with  $dCor(F_X(X), F_Y(Y))$  by transforming the data to ranks, and with  $dCor(\Phi^{-1}(F_X(X)), \Phi^{-1}(F_Y(Y)))$  using coordinatewise normal scores.

To thoroughly compare the methods we use 16 data settings. We consider 10 bivariate settings, based on Chaudhuri and Hu (2019) and Reshef et al. (2018). In addition we study 6 multivariate settings, following the simulation in Székely et al. (2007). An overview of the bivariate simulation settings is given in Figure 8. For each setting we generate 2000 samples according to the specified distributions. On each of these samples, we then execute a permutation test with  $\lfloor (200 + 5000/n) \rfloor$  permutations and a significance level of 0.1 as in Székely et al. (2007).

We first discuss the results of the bivariate settings. We present the most interesting results here, and refer to Section E of the Supplementary Material for the results on the other settings, which gave more moderate and qualitatively similar results. Figure 9 shows the results of the power simulation on the quadratic, square, cosine and circle setups. We see that all methods perform reasonably well and usually achieve a high power for sample sizes of  $n = 100$  and upwards. An exception is the circle setup, where all methods require a higher sample size to achieve a satisfactory power level. Interestingly, the classical dCor performs worst here, with the dCor after rank transform as a second. The biloop dCor and dCor after normal scores perform similarly and are on top.

Figure 10 summarizes the multivariate settings. The power for the first four of these, with Gaussian data and various multivariate  $t$ -distributions, is plotted in Figure 11.

For all methods, heavier tails led to higher power. This is because most methods give more weight to points further away from the center, which makes them more sensitive to dependence in the tails. This explanation is confirmed by the fact that dCor typically performs somewhat better than the other alternatives here. Its non-robustness causes it to easily pick up the dependence in the extreme tails of the distributions. Normal scores is next, and is also sensitive to dependence in the tails due to the unboundedness of the applied transformation. The biloop transform is ranked third here, and still performs well even though its robustness properties make it less dependent on the tails of the distribution. The dCor after rank transform performed only slightly lower.

Figure 12 plots the power of the permutation tests on the multiplicative and log-squared settings. In the multiplicative setting dCor performed best, followed by the normal scores, biloop, and rank transforms. Note that this is again a setup where the dependence is most pronounced in the tails. In the log-squared setting we have more dependence in the center of the distribution. Here the biloop together with normal scores performed best. The rank

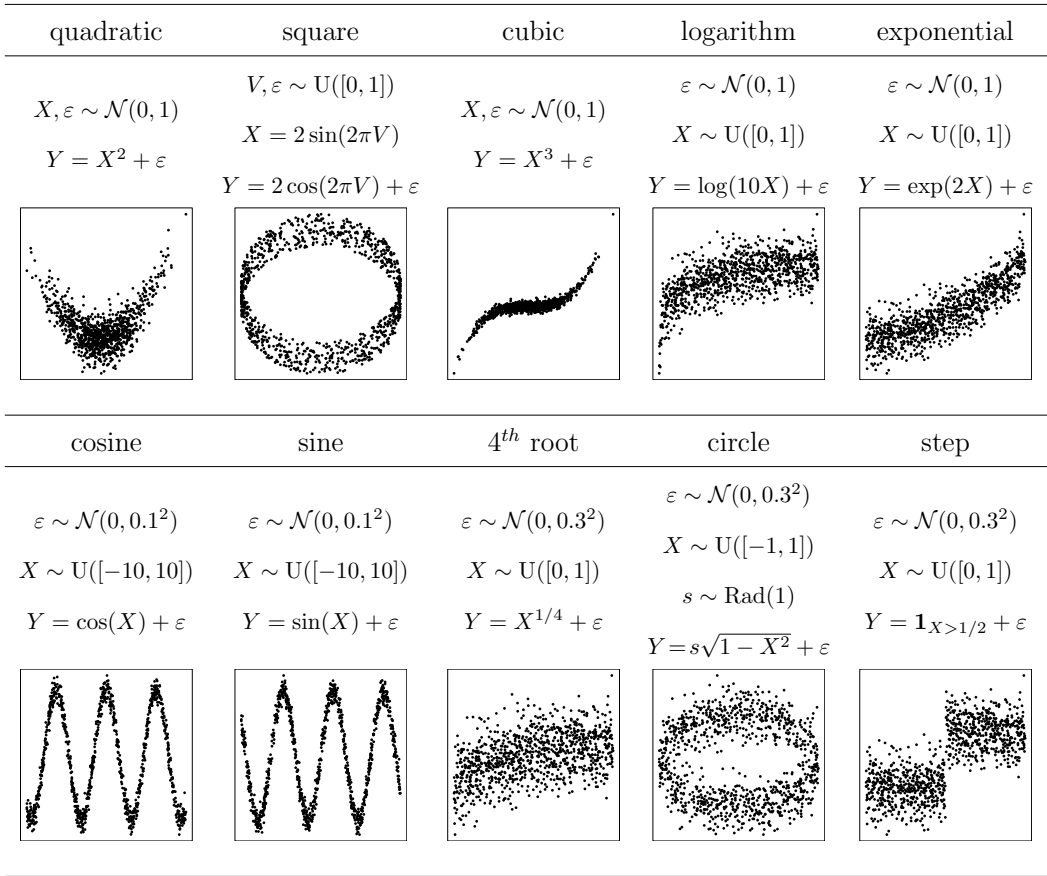


FIGURE 8 The bivariate settings for the power simulation.

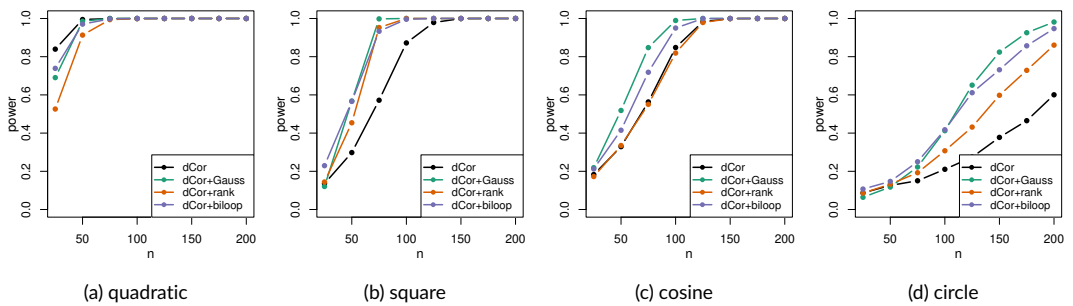
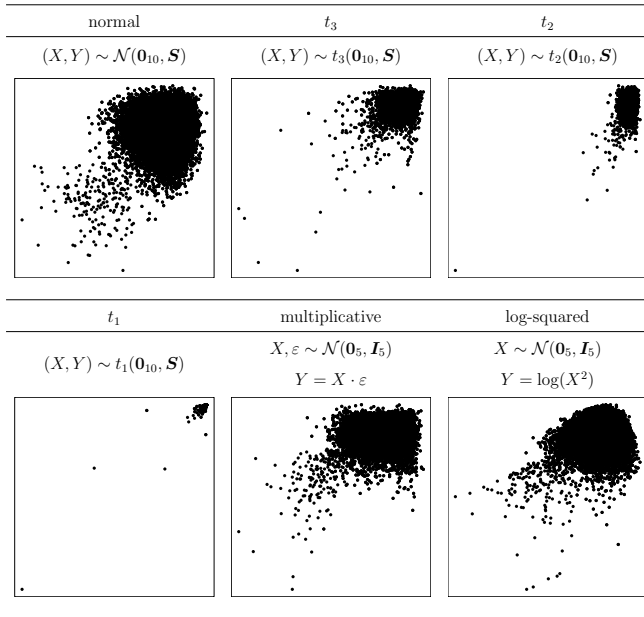
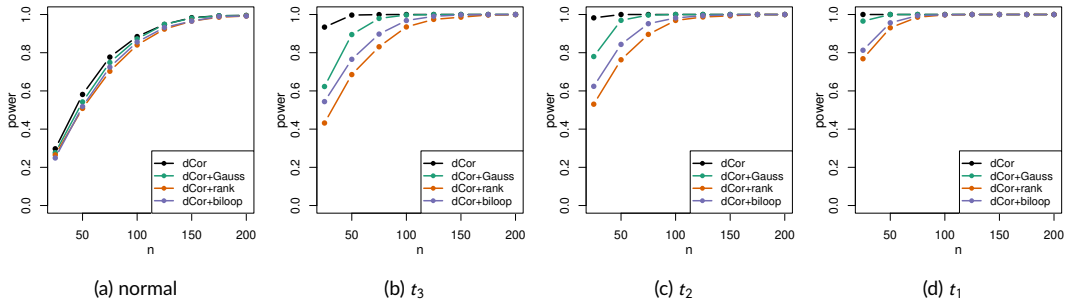


FIGURE 9 Results of the power simulation on bivariate  $(X, Y)$  for different sample sizes  $n$ .

transform still performed quite well, followed by the classical dCor.



**FIGURE 10** Plots of doubly centered distances of  $Y$  versus those of  $X$  for the settings of the power simulation, where  $S = \begin{bmatrix} I_5 & 1_5 1_5^T / 10 \\ 1_5 1_5^T / 10 & I_5 \end{bmatrix}$ .



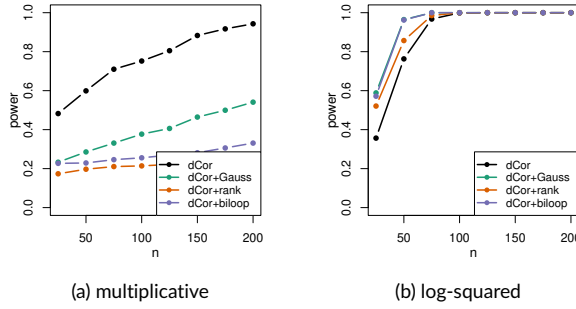
**FIGURE 11** Power simulation in the multivariate normal,  $t_3$ ,  $t_2$  and  $t_1$  settings.

## 5.2 | Robustness simulation

We now explore the robustness of the various dependence measures to contamination. The clean data are samples of size  $n = 500$  from  $(X, Y) \sim \mathcal{N}_2\left(\begin{bmatrix} 0 \\ 0 \end{bmatrix}, \begin{bmatrix} 1 & \rho \\ \rho & 1 \end{bmatrix}\right)$ , with  $\rho$  either 0 or 0.6. We then replace a fraction  $\varepsilon$  of the generated points by outliers.

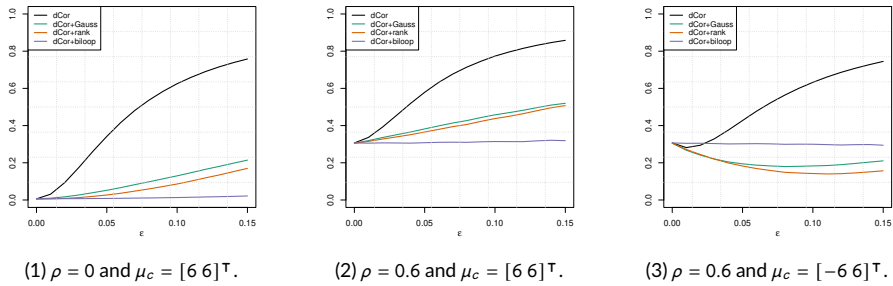
We first consider contamination generated as a small cloud of  $\varepsilon n$  points following the distribution  $\mathcal{N}_2(\mu_c, 0.25I_2)$ . For  $\rho = 0$  we take  $\mu_c = [6 \ 6]^T$ , whereas for  $\rho = 0.6$  we consider  $\mu_c = [6 \ 6]^T$  and  $\mu_c = [-6 \ 6]^T$ .

Figure 13 shows the average values of the different dependence measures for increasing levels of contamination. Note that we correct the dependence measures such that they estimate the same population quantity on the clean



**FIGURE 12** Power simulation in the multivariate settings multiplicative and log-squared.

distribution by multiplying with the consistency factor  $c_\psi = \text{dCor}(X, Y) / \text{dCor}(\psi(X), \psi(Y))$ . The pattern is quite similar in all three situations. The original dCor is most strongly affected by the contamination. If dCor is applied after normal scores or the rank transform, it is less affected by the contamination. The biloop dCor is barely affected.



**FIGURE 13** Robustness against 100ε% of outliers.

Next we consider the same distributions for the clean data, but this time we add 5% outliers and vary their distance from the origin. We take the values of the outliers to be  $\mu_c = [x \ x]^T$  for  $\rho = 0$ , and  $\mu_c = [x \ x]^T$  or  $\mu_c = [x \ -x]^T$  for  $\rho = 0.6$ . Figure 14 shows the results of this setup as a function of  $x$ . These results confirm what we expected from Section 3. The original dCor has an unbounded sensitivity curve, which converges to its bounded influence function for growing sample size. In this simulation the sample size is fixed, so the curve deviates as the contamination moves further away from the center. The other three dependence measures are much less affected.

### 5.3 | Rejection of independence under contamination

We now investigate the effect of contamination when the clean distribution has independence. More precisely, we investigate how often the null hypothesis of independence is falsely rejected when adding contamination to the clean data. The clean data is generated similarly to the setting used in Table 1 of Székely et al. (2007). We sample  $(X, Y)$  from the independent bivariate standard normal,  $t_3$ ,  $t_2$ , and  $t_1$  distributions. We perform permutation tests as in Section 5.1, at a significance level of 0.1 and with  $\lfloor 5000/n + 200 \rfloor$  permutations.

First, we consider clean distributions plus a lone outlier  $[x \ x]^T$ . The sample size is fixed at  $n = 200$ . In Figure 15 the single outlier has a strong effect on the classical dCor, whereas the other independence measures stay almost

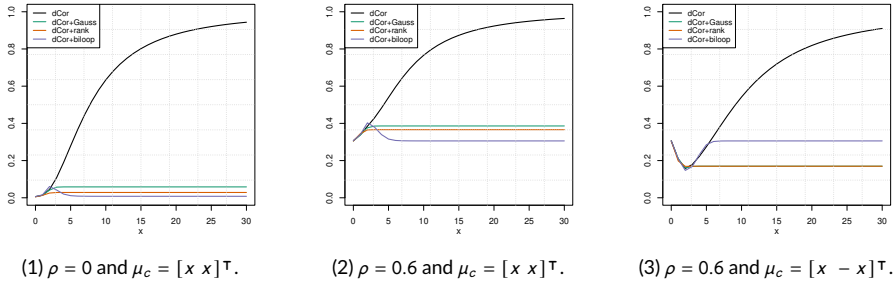


**FIGURE 14** Robustness against 5% of outliers for varying degrees of outlyingness.

unaltered. The distortion is most pronounced for the lighter tailed normal distribution. The effect dies out as we move towards the  $t_1$  distribution, as the size of the outlier becomes small relative to the clean observations in the tails, so its influence diminishes.

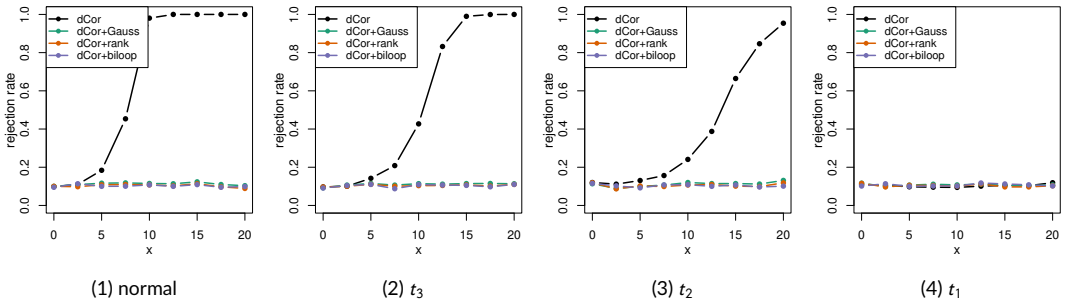


**FIGURE 15** Rejection rates of the permutation tests when one outlier is added in  $[x \ x]^T$ .

Figure 16 shows results for the same setup, but now with 5% of contamination in  $[x \ x]^T$ . This time the tests are affected more quickly when  $x$  starts to grow. The effect is delayed for heavier-tailed distributions, for the same reason as before. The biloop dCor shows its unique redescending nature, as the rejection rate returns to approximately 10% for very large  $x$ . Interestingly, for the  $t_1$  distribution it is the classical dCor whose rejection rate grows the slowest when  $x$  increases. This is again explained by the fact that, among the measures considered, the classical dCor assigns the most weight to the tails, and the tails of the  $t_1$  distribution dominate the size of the outliers.

Instead of focusing on the effect of increasing outlyingness, we now focus on the effect of increasing contamination level. We consider the same normal,  $t_3$ ,  $t_2$ , and  $t_1$  distributions for the clean data, with  $n = 200$ . We now contaminate by a fraction  $\varepsilon$  of outliers sampled from  $\mathcal{N}_2([6 \ 6]^T, 0.25 \mathbf{I}_2)$ . Figure 17 shows the rejection rates of the different permutation tests as a function of  $\varepsilon$ . The curves clearly indicate that the measures assign a different importance to the tails. The original dCor is the most sensitive to them (except at the long-tailed  $t_1$  distribution), followed by the normal scores and the rank transform. The biloop dCor is the least sensitive to the tails.

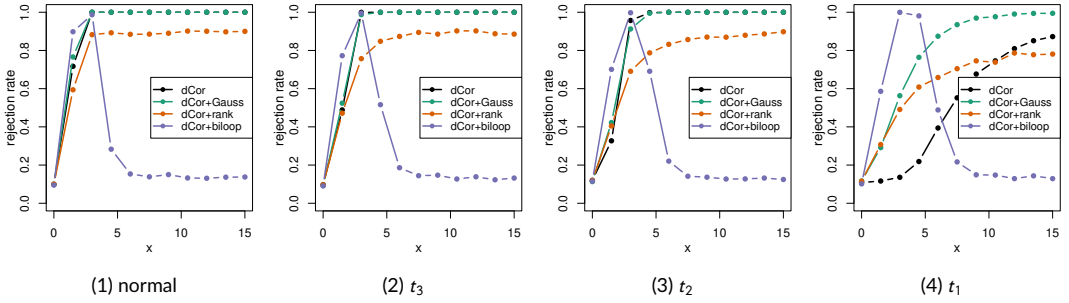


FIGURE 16 Rejection rates for 5% of outliers in  $[x \ x]^T$ .

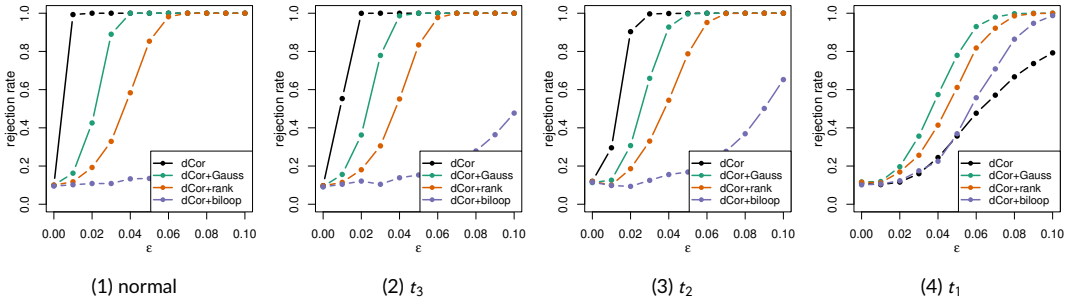


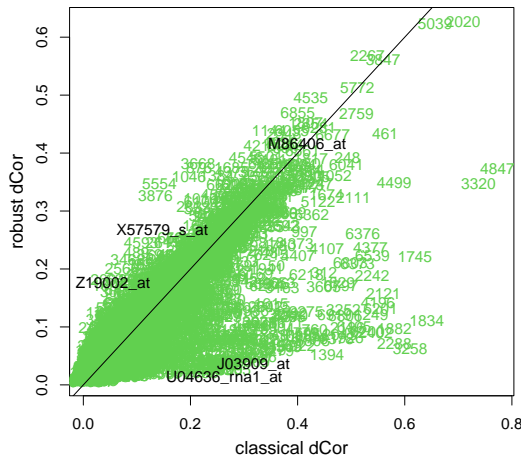
FIGURE 17 Rejection rates for 100ε% of outliers.

## 6 | REAL DATA EXAMPLE

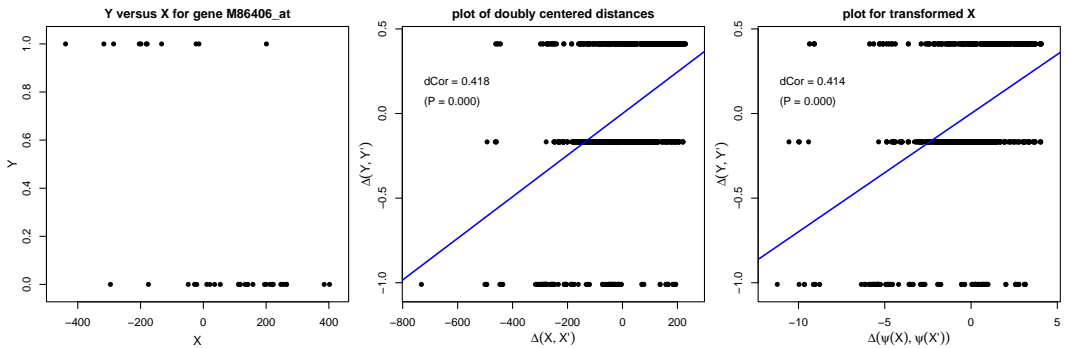
As an illustration we consider a data set originating from Golub et al. (1999), who aimed to distinguish between two types of acute leukemia on the basis of microarray evidence. The input data is a matrix  $X$  whose  $n = 38$  rows correspond to the patients, and with  $p = 7,129$  columns corresponding to the genes. The binary response vector  $Y$  takes on the value 0 for the 27 patients with leukemia type ALL and 1 for the 11 patients with type AML. The data was previously analyzed by Hall and Miller (2009). Here our purpose is to study dependence of general type between the variables (genes)  $X^j$  and the response  $Y$ .

Figure 18 plots the biloop dCor versus the classical dCor. The light colored numbers inside the plot are the values of  $j$ , the number of the gene. Most of the points are concentrated around the main diagonal, so for them both versions of dCor are close together.

As an example we look at gene M86406\_at corresponding to  $j = 2301$ , which has high values for both as seen in Figure 18. The leftmost panel of Figure 19 is simply a plot of  $Y$  versus  $X^j$ . This indicates a kind of decreasing relation, as would also be detected by a rank correlation. The middle panel is a plot of the doubly centered (DC) distances  $\Delta(Y, Y')$  of  $Y$  versus the DC distances  $\Delta(X^j, (X^j)')$  of  $X^j$ . This plot contains  $38^2/2 = 722$  points (instead of 38). We note that the DC distances of  $Y$  take only three values. This is because  $Y$  itself is binary. It can easily be verified that the pairs  $(y_j, y_k)$  with  $y_j = 1 = y_k$  yield the lowest of the three values, and the pairs with  $y_j = 0 = y_k$  yield the middle value. The pairs for which  $y_j \neq y_k$  obtain the top value. If the response  $Y$  had an equal number of zeroes and ones, the pairs  $(0, 0)$  and  $(1, 1)$  would all obtain the same value  $-0.5$ , and the pairs with differing response would obtain 0.5.



**FIGURE 18** Leukemia data: plot of robust dCor versus classical dCor for all genes.



**FIGURE 19** Gene M86406\_at of the leukemia data, with  $j = 2301$ . Left: plot of  $Y$  versus  $X^j$ . Middle: doubly centered distances  $\Delta(Y, Y')$  of  $Y$  versus those of  $X^j$ . Right: versus those of  $\psi_\infty(X^j)$ .

The distance correlation of 0.418 equals the Pearson correlation between the DC distances of  $X^j$  and those of  $Y$ . It is highly significant, with  $p$ -value computed as 0.000 by the permutation test using 10,000 permutations. The panel also contains the least squares regression line computed from these points, which is also related to the dCor, and visualizes the strength of the relation. Note that the DC distances of  $Y$  and  $X^j$  do not follow a linear model, but that is not necessary since the Pearson correlation arises here for a different mathematical reason.

The right hand panel of Figure 19 plots the DC distances of  $Y$  versus those of the transformed variable  $\psi_\infty(X^j)$ . This yields the robustified version of dCor, given as 0.414 which is again highly significant. The pattern in this plot is quite similar to that in the previous plot, since the variable  $X^j$  did not contain outliers. Note that the scale of the DC distances  $\Delta(\psi_\infty(X^j), (\psi_\infty(X^j))')$  on the horizontal axis is totally different from that of the original  $\Delta(X^j, (X^j)')$ , because the transformation  $\psi_\infty$  contains a standardization. This does not matter, because the Pearson correlation is invariant to rescaling, so dCor is too. Also note that we did not transform  $Y$  in the same way. That is because  $\psi_\infty(Y)$  would take only two values, so its DC distances would simply be a rescaled version of those of  $Y$  itself, and therefore

yield exactly the same dCor.

We are also interested in genes for which the classical and the robustified dCor are quite different. We first look at an example where the robustified dCor is much lower than the classical one. For this purpose we restricted attention to the genes with robust dCor below 0.05, and among those we looked for the largest value of classical minus robust. This occurs for  $j = 1092$ , which is the gene J03909\_at indicated in Figure 18. The top left panel of Figure 20 plots  $Y$  versus  $X^j$ . We immediately note that there are several points with outlying values of  $X^j$  on the right. Their  $x_{ij}$  lie far away relative to the scale of the remaining  $x_{ik}$ . These patients all belong to the same class with  $y_i = 1$ .

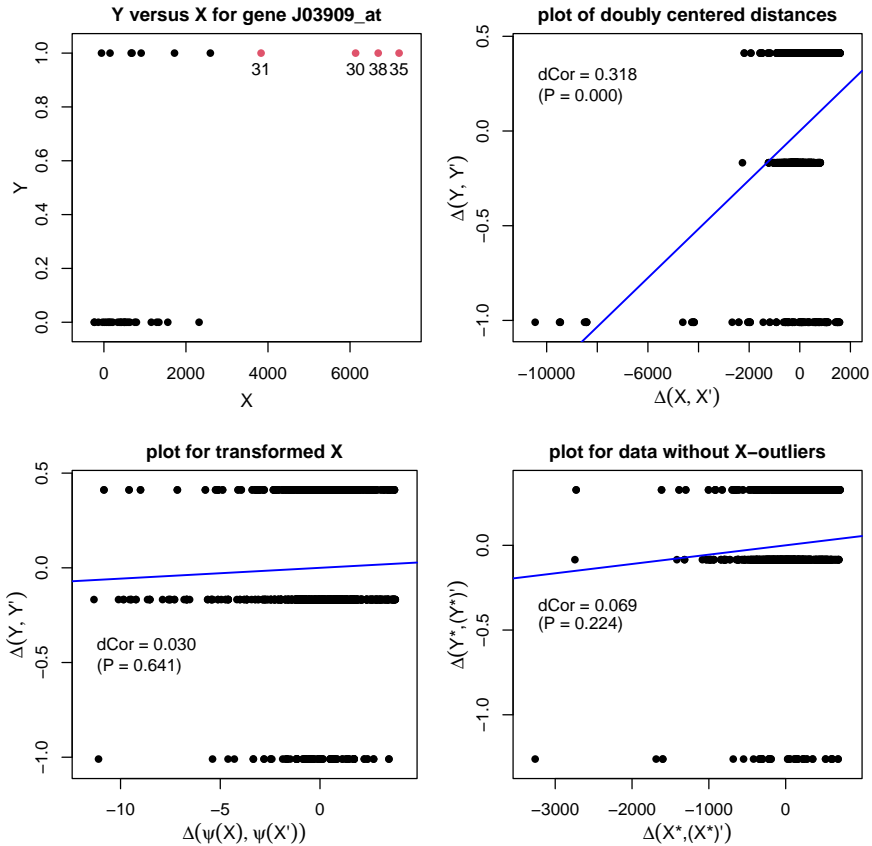


**FIGURE 20** Gene J03909\_at of the leukemia data ( $j = 1092$ ). Top left: plot of  $Y$  versus  $X^j$ , with the four outliers. Top right: doubly centered distances  $\Delta(Y, Y')$  of  $Y$  versus those of  $X^j$ . Bottom left:  $\Delta(Y, Y')$  versus doubly centered distances of  $\psi_\infty(X^j)$ . Bottom right: plot of doubly centered distances of the data  $((X^j)^*, Y^*)$  without the outliers.

The top right panel of Figure 20 plots the DC distances of  $Y$  versus those of  $X^j$ . We see that  $\Delta(X^j, (X^j)')$  has far outliers on the left hand side, which are due to the outliers in  $X^j$ . Those outliers were on the right hand side, but that direction does not matter as a mirror image of  $X^j$  yields the same DC distances since  $\Delta(-X^j, (-X^j)') = \Delta(X^j, (X^j)')$ . The distance correlation of 0.318 is highly significant with  $p$ -value around 0.000. The regression line is indeed quite steep, its slope being determined mainly by the leverage of the outliers on the left.

In the bottom left panel we see the corresponding plot with the transformed variable  $\psi_\infty(X)$ . The  $\Delta(\psi_\infty(X^j), (\psi_\infty(X^j))')$  still have a longer tail on the left than on the right, but there are no extreme outliers as in the previous panel. Now dCor is very low, with an insignificant p-value.

Finally, the bottom right panel shows what happens if we remove the four points with outlying  $x$ -values, yielding a reduced dataset denoted as  $(X^*, Y^*)$  in the plot. The dCor is again quite low and insignificant. Indeed, if we remove the labeled points in the top left panel there appears to be little structure left. Applying the robust dCor or taking out the outliers gives similar results here. This is an example where most of the information about the dependence between  $X^j$  and  $Y$  is in the tails of the data, so it is reflected in the classical dCor and not in its more robust version. The difference between the classical and the robust dCor thus points our attention to the fact that the conclusion rests heavily on these four cases. Afterward it is up to the user to find out whether these  $x$ -values are correct or may be due to errors. In this dataset, measured by sophisticated equipment, they may well be correct.

The gene with the second largest difference classical - robust has  $j = 5376$ . It is analyzed in Section F of the Supplementary Material.

Finally, we also want to look at an example where the robust dCor is higher than the classical one. We looked at some genes where the difference robust - classical was high, and for illustration purposes we selected a simple one with only a single outlier. Figure 21 shows the analysis for gene Z19002\_at with  $j = 5071$ .

In the top left panel of Figure 21 we see that patient 26 has a very outlying value of  $X^j$ . This outlier yields a single far outlier in the top right panel, because the other DC distances involving patient 26 turn out to be not nearly as far away. It may seem strange that there is only one DC distance from case 26 standing out, but this agrees nicely with the proof of the breakdown value in Section C.1 of the Supplementary Material, indicating that the DC distance of the outlier to itself (denoted there as  $\Delta_{11}$ ) dominates all others. The low distance correlation of 0.055 is not significant at all. But in the bottom left plot we see that the use of the transformation  $\psi_\infty$  has brought the outlier much closer, thereby greatly reducing its effect. The robust dCor increases to 0.175 and becomes significant. Also, taking out the outlier entirely yields the bottom right plot which has a similar pattern. So removing the single outlier brings the classical dCor closer to the robust one. (If one applies the robust dCor to the reduced data set, it barely changes.)

## 7 | OUTLOOK

The distance correlation is increasingly being adopted by different scientific disciplines. Martínez-Gómez et al. (2014) identified new nonlinear dependencies between astrophysical variables by dCor, and found it worked better than the maximal correlation coefficient. In biology, Lin et al. (2022) computed dCor between microbe taxa, using sparse and compositional data. Among medical applications, Kong et al. (2012) computed dCor between four variables: lifestyle, pedigree, disease, and mortality, some of which were multivariate so they can be seen as groups of variables. Geerligs et al. (2016) identified functional connectivity between regions of the human brain by applying dCor to higher-dimensional variables. In genomics, Guo et al. (2014) searched for nonlinear relationships in gene expression data in order to detect gene regulation, and found that dCor was better suited for this purpose than mutual information. Broadaway et al. (2016) used dCov to detect genetic variations (genotypes) that affect several traits (phenotypes) simultaneously.

While distance correlation has become a popular tool in statistical practice, its behavior in the presence of outliers has received relatively little attention. One of the reasons may be that it is not obvious how to measure dependence robustly, which is the issue that we address here. Therefore, we hope that our work will lead to a better understanding of the behavior of dCov and dCor under contamination, and that the version using the biloop transform will help to

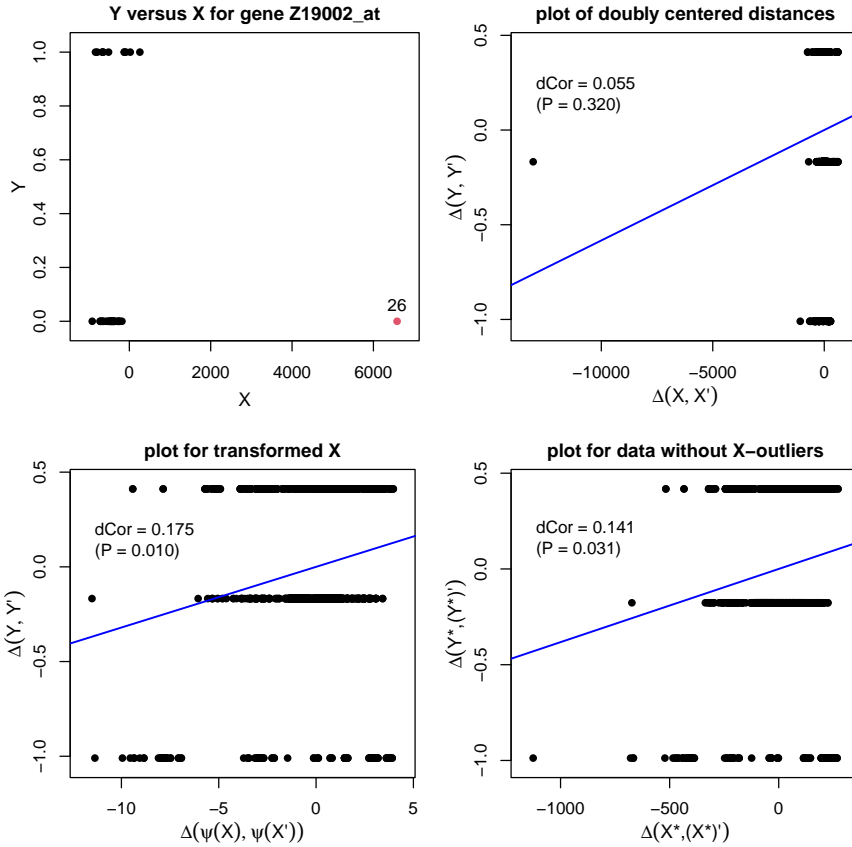


**FIGURE 21** The panels are as in Figure 20, but for gene Z19002\_at ( $j = 5071$ ).

detect additional dependencies, as well as point out some dependencies are concentrated in the tails.

Our work may also lead to new methodological development. The distance correlation, and independence measures in general, have seen a surge in research attention over the last two decades. For instance, various connections were found between distance covariance and Brownian motion (Székely and Rizzo, 2009), as well as with the Hilbert-Schmidt Independence Criterion (HSIC) of Gretton et al. (2005) (Sejdinovic et al., 2013) and with so-called global tests (Edelmann and Goeman, 2022). Much of the current interest in measures of general dependence is driven by novel and impactful methodological advances which rely on them. We present a brief overview of these methodologies here.

Feature selection is a statistical challenge for which general dependence measures have been leveraged successfully. With the increasing popularity of nonlinear models in both statistics and machine learning, selecting features based on linear dependence measures is insufficient. Capturing general dependence allows for feature selection which caters to the use of more complex models in a second step. Li et al. (2012) used dCor for this, as did we in our real data example, whereas Song et al. (2012) applied the HSIC. Kong et al. (2015) applied dCov to feature selection with a high number of regressors by means of a sure independence screening approach, with applications to genetic data. Kong et al. (2017) used dCor to search for interaction terms. Vepakomma et al. (2018) employed dCor to construct a

small set of latent regressors.

Independent component analysis (ICA) aims to construct a set of independent sources that together explain the observed nongaussian multivariate dataset. It is frequently used, e.g. in blind source separation. Matteson and Tsay (2017) developed a new ICA algorithm based on dCov. We are currently working on an extension based on the more robust variant of dCov proposed here.

A key area where measuring independence is a fundamental building block is causal inference, and causal discovery in particular. In causal discovery, the goal is to identify a structural equation model and the underlying directed acyclic graph (DAG) from observational data. Under appropriate assumptions on the model classes and noise distributions, this can be done. However, inferring which DAGs can give rise to a given observational distribution can only be done by relying on general dependence measures. For this purpose Zhang et al. (2011) constructed a conditional independence test by means of an extension of the HSIC. Pfister et al. (2018) extended HSIC to test for joint independence of variables. Runge et al. (2019) employed dCor, and Leyder et al. (2024) used both HSIC and dCor.

The machine learning community has adopted general dependence measures in several other methods. Measuring general dependence is often used to quantify a (dis)similarity between distributions or representations, without relying on particular distributional assumptions or linearity. An important task is measuring the similarity of networks. Measuring similarities between different deep neural network (NN) representations is an important step in understanding the inner workings of these networks. Kornblith et al. (2019) introduce independence-based measures of NN similarity called centered kernel alignment (CKA), which reveal connections between network width and the sensitivity to training initialization.

In transfer component analysis (Pan et al., 2010), the goal is to use data in a source domain to build models that perform well in a different but related target domain. Typically, the strategy is to find a representation of the data that is similar in both domains. As in CKA, no distributional or linearity assumptions are made, which is why general independence measures are preferred to quantify similarity (Xiao and Guo, 2014; Yan et al., 2017). Other machine learning applications include clustering (Niu et al., 2010; Cao et al., 2015; Wang et al., 2019), convolutional neural networks (Wang et al., 2020), and learning de-biased representations (Bahng et al., 2020).

## 8 | CONCLUSIONS

The distance covariance dCov of Székely et al. (2007) is a popular measure of dependence between real random variables, because it addresses all forms of dependence rather than only linear or monotone relations. Its simple definition is an added benefit. Various claims have been made in the literature about its robustness to outliers, but this aspect was not yet studied in detail.

In this paper we have investigated the robustness properties of dCov, as well as the distance variance and the distance correlation, by deriving influence functions and breakdown values. This led to the surprising result that the influence function of the usual distance covariance is bounded, but that its breakdown value is zero. The unbounded sensitivity function converges to the bounded influence function for increasing sample size. The robustness of dCor is thus not quite as high as expected. This led us to the construction of a more robust version based on the biloop, a novel data transformation. The new version held its own in simulations and was illustrated on a genetic dataset, where comparing the classical dCor with its more robust version provided additional insight in the data. In the outlook section we noted that there are many application areas of dCov and dCor in which the robust version could be useful.

**Acknowledgment.** Thanks go to the Editor and reviewers for helpful comments that improved the presentation.

**Software availability.** The dataset of the example and an R script reproducing the results are available at <https://wis.kuleuven.be/statdatascience/robust/software>.

## References

- Andrews, D. F., P. J. Bickel, F. R. Hampel, P. J. Huber, W. H. Rogers, and J. W. Tukey (1972). *Robust Estimates of Location: Survey and Advances*. Princeton University Press.
- Bahng, H., S. Chun, S. Yun, J. Choo, and S. J. Oh (2020). Learning de-biased representations with biased representations. In *International Conference on Machine Learning*, pp. 528–539. PMLR.
- Beaton, A. E. and J. W. Tukey (1974). The fitting of power series, meaning polynomials, illustrated on band-spectroscopic data. *Technometrics* 16(2), 147–185.
- Boudt, K., J. Cornelissen, and C. Croux (2012). The gaussian rank correlation estimator: robustness properties. *Statistics and Computing* 22(2), 471–483.
- Broadaway, K. A., D. J. Cutler, R. Duncan, J. L. Moore, E. B. Ware, M. A. Jhun, L. F. Bielak, W. Zhao, J. A. Smith, P. A. Peyser, et al. (2016). A statistical approach for testing cross-phenotype effects of rare variants. *The American Journal of Human Genetics* 98(3), 525–540.
- Cao, X., C. Zhang, H. Fu, S. Liu, and H. Zhang (2015). Diversity-induced multi-view subspace clustering. In *Proceedings of the IEEE conference on computer vision and pattern recognition*, pp. 586–594.
- Chaudhuri, A. and W. Hu (2019). A fast algorithm for computing distance correlation. *Computational Statistics & Data Analysis* 135, 15–24.
- Chen, X., X. Chen, and H. Wang (2018). Robust feature screening for ultra-high dimensional right censored data via distance correlation. *Computational Statistics & Data Analysis* 119, 118–138.
- Davis, R. A., M. Matsui, T. Mikosch, and P. Wan (2018). Applications of distance correlation to time series. *Bernoulli* 24, 3087–3116.
- Donoho, D. L. and P. J. Huber (1983). The notion of breakdown point. In P. Bickel, K. Doksum, and J. L. Hodges (Eds.), *A Festschrift for Erich L. Lehmann*, pp. 157–184. Belmont, Wadsworth.
- Edelmann, D. and J. Goeman (2022). A Regression Perspective on Generalized Distance Covariance and the Hilbert–Schmidt Independence Criterion. *Statistical Science* 37, 562–579.
- Geerligs, L., R. N. Henson, et al. (2016). Functional connectivity and structural covariance between regions of interest can be measured more accurately using multivariate distance correlation. *NeuroImage* 135, 16–31.
- Golub, T. R., D. K. Slonim, P. Tamayo, C. Huard, M. Gassenbeek, J. P. Mesirov, H. Coller, M. L. Loh, J. R. Downing, M. A. Caligiuri, C. D. Bloomfield, and E. S. Lander (1999). Molecular classification of cancer: Class discovery and class prediction by gene expression monitoring. *Science* 286, 531–537.
- Gretton, A., R. Herbrich, A. Smola, O. Bousquet, B. Schölkopf, and A. Hyvärinen (2005). Kernel methods for measuring independence. *Journal of Machine Learning Research* 6(12), 2075–2129.
- Guo, X., Y. Zhang, W. Hu, H. Tan, and X. Wang (2014). Inferring nonlinear gene regulatory networks from gene expression data based on distance correlation. *PLoS one* 9(2), e87446.

- Hall, P. and H. Miller (2009). Using Generalized Correlation to Effect Variable Selection in Very High Dimensional Problems. *Journal of Graphical and Computational Statistics* 18(3), 533–550.
- Hampel, F. R., E. M. Ronchetti, P. J. Rousseeuw, and W. A. Stahel (1986). *Robust Statistics: The Approach Based on Influence Functions*. New York: Wiley.
- Huo, X. and G. J. Székely (2016). Fast Computing for Distance Covariance. *Technometrics* 58, 435–447.
- Kasieczka, G. and D. Shih (2020). Robust Jet Classifiers through Distance Correlation. *Physical Review Letters* 125, 122001.
- Kong, J., B. E. Klein, R. Klein, K. E. Lee, and G. Wahba (2012). Using distance correlation and ss-anova to assess associations of familial relationships, lifestyle factors, diseases, and mortality. *Proceedings of the National Academy of Sciences* 109(50), 20352–20357.
- Kong, J., S. Wang, and G. Wahba (2015). Using distance covariance for improved variable selection with application to learning genetic risk models. *Statistics in medicine* 34(10), 1708–1720.
- Kong, Y., D. Li, Y. Fan, and J. Lv (2017). Interaction pursuit in high-dimensional multi-response regression via distance correlation. *The Annals of Statistics* 45(2), 897 – 922.
- Kornblith, S., M. Norouzi, H. Lee, and G. Hinton (2019). Similarity of neural network representations revisited. In *International conference on machine learning*, pp. 3519–3529. PMLR.
- Leyder, S., J. Raymaekers, and T. Verdonck (2024). TSLiNGAM: DirectLiNGAM under heavy tails. *Journal of Computational and Graphical Statistics*, appeared online, <https://doi.org/10.1080/10618600.2024.2394462>.
- Li, R., W. Zhong, and L. Zhu (2012). Feature screening via distance correlation learning. *Journal of the American Statistical Association* 107(499), 1129–1139.
- Lin, H., M. Eggesbø, and S. D. Peddada (2022). Linear and nonlinear correlation estimators unveil undescribed taxa interactions in microbiome data. *Nature communications* 13(1), 4946.
- Mai, Q., D. He, and H. Zou (2023). Coordinate-wise Gaussianization: Theories and Applications. *Journal of the American Statistical Association* 118(544), 2329–2343.
- Martínez-Gómez, E., M. T. Richards, and D. S. P. Richards (2014). Distance correlation methods for discovering associations in large astrophysical databases. *The Astrophysical Journal* 781(1), 39.
- Matteson, D. S. and R. S. Tsay (2017). Independent Component Analysis via Distance Covariance. *Journal of the American Statistical Association* 112(518), 623–637.
- Niu, D., J. G. Dy, and M. I. Jordan (2010). Multiple non-redundant spectral clustering views. In *Proceedings of the 27th international conference on machine learning (ICML-10)*, pp. 831–838.
- Pan, S. J., I. W. Tsang, J. T. Kwok, and Q. Yang (2010). Domain adaptation via transfer component analysis. *IEEE transactions on neural networks* 22(2), 199–210.
- Pfister, N., P. Bühlmann, B. Schölkopf, and J. Peters (2018). Kernel-based tests for joint independence. *Journal of the Royal Statistical Society Series B: Statistical Methodology* 80(1), 5–31.
- Raymaekers, J. and P. J. Rousseeuw (2021). Fast Robust Correlation for High-Dimensional Data. *Technometrics* 63(2), 184–198.
- Raymaekers, J. and P. J. Rousseeuw (2025). Distance Covariance, Independence, and Pairwise Differences. *The American Statistician* 79(1), 122–128.
- Reshef, D. N., Y. A. Reshef, P. C. Sabeti, and M. Mitzenmacher (2018). An empirical study of the maximal and total information coefficients and leading measures of dependence. *The Annals of Applied Statistics* 12(1), 123 – 155.

- Runge, J., P. Nowack, M. Kretschmer, S. Flaxman, and D. Sejdinovic (2019). Detecting and quantifying causal associations in large nonlinear time series datasets. *Science advances* 5(11), eaa4996.
- Sejdinovic, D., G. Sriperumbudur, A. Gretton, and K. Fukumizu (2013). Equivalence of distance-based and RKHS-based statistics in hypothesis testing. *The Annals of Statistics* 41, 2263–2291.
- Song, L., A. Smola, A. Gretton, J. Bedo, and K. Borgwardt (2012). Feature selection via dependence maximization. *Journal of Machine Learning Research* 13(5), 1393–1434.
- Székely, G. J. and M. L. Rizzo (2009). Brownian distance covariance. *The Annals of Applied Statistics* 3(4), 1236–1265.
- Székely, G. J. and M. L. Rizzo (2012). On the uniqueness of distance covariance. *Statistics & Probability Letters* 82(12), 2278–2282.
- Székely, G. J. and M. L. Rizzo (2023). *The Energy of Data and Distance Correlation*. Chapman & Hall.
- Székely, G. J., M. L. Rizzo, and N. K. Bakirov (2007). Measuring and testing dependence by correlation of distances. *The Annals of Statistics* 35(6), 2769–2794.
- Ugwu, S., P. Miasnikof, and Y. Lawryshyn (2023). Distance correlation market graph: The case of S&P500 stocks. *Mathematics* 11(18), 3832.
- Vepakomma, P., C. Tonde, and A. Elgammal (2018). Supervised dimensionality reduction via distance correlation maximization. *Electronic Journal of Statistics* 12(1), 960 – 984.
- Wang, X., Z. Lei, X. Guo, C. Zhang, H. Shi, and S. Z. Li (2019). Multi-view subspace clustering with intactness-aware similarity. *Pattern Recognition* 88, 50–63.
- Wang, X., M. Zhu, D. Bo, P. Cui, C. Shi, and J. Pei (2020). Am-gcn: Adaptive multi-channel graph convolutional networks. In *Proceedings of the 26th ACM SIGKDD International conference on knowledge discovery & data mining*, pp. 1243–1253.
- Xiao, M. and Y. Guo (2014). Feature space independent semi-supervised domain adaptation via kernel matching. *IEEE transactions on pattern analysis and machine intelligence* 37(1), 54–66.
- Yan, K., L. Kou, and D. Zhang (2017). Learning domain-invariant subspace using domain features and independence maximization. *IEEE transactions on cybernetics* 48(1), 288–299.
- Zhang, K., J. Peters, D. Janzing, and B. Schölkopf (2011). Kernel-based conditional independence test and application in causal discovery. In *Proceedings of the Twenty-Seventh Conference on Uncertainty in Artificial Intelligence, UAI'11*, Arlington, Virginia, USA, pp. 804–813. AUAI Press.
- Zhang, Q. (2019). Independence test for large sparse contingency tables based on distance correlation. *Statistics & Probability Letters* 148, 17–22.
- Zhou, Z. (2012). Measuring nonlinear dependence in time-series, a distance correlation approach. *Journal of Time Series Analysis* 33(3), 438–457.

## Supplementary Material

### A | PROOFS OF THE INFLUENCE FUNCTIONS OF SECTION 2

#### A.1 | Proofs of Section 2.1

**Proof of Proposition 1** For the sake of simplifying notation, we exclude the exponent  $\alpha$  since the proof remains unchanged. We proceed as follows. Let  $(X_\varepsilon, Y_\varepsilon) \sim F_{X,Y}^\varepsilon = (1 - \varepsilon)F_{X,Y} + \varepsilon\Delta_{(s,t)}$ . Then

$$d\text{Cov}(X_\varepsilon, Y_\varepsilon) = \underbrace{\mathbb{E}[|X_\varepsilon - X'_\varepsilon| | Y_\varepsilon - Y'_\varepsilon]}_{(1)} + \underbrace{\mathbb{E}[|X_\varepsilon - X'_\varepsilon|] \mathbb{E}[|Y_\varepsilon - Y'_\varepsilon|]}_{(2)} - 2 \underbrace{\mathbb{E}[|X_\varepsilon - X'_\varepsilon| | Y_\varepsilon - Y''_\varepsilon]}_{(3)}.$$

For the first term, we obtain:

$$\begin{aligned} \mathbb{E}[|X_\varepsilon - X'_\varepsilon| | Y_\varepsilon - Y'_\varepsilon] &= \int |x - x'| |y - y'| \underbrace{f_{XY}^\varepsilon(x, y) f_{XY}^\varepsilon(x', y')}_{=(1-\varepsilon)^2 f_{XY}(x, y) f_{XY}(x', y') + \varepsilon^2 \Delta_{s,t} \Delta_{s,t} + \varepsilon(1-\varepsilon) f_{XY}(x, y) \Delta_{s,t} + (1-\varepsilon)\varepsilon \Delta_{s,t} f_{XY}(x', y')} dx dx' dy dy' \\ &= (1 - \varepsilon)^2 \mathbb{E}[|X - X'| | Y - Y'] + \varepsilon^2 (|s - s| | t - t|) \\ &\quad + \varepsilon(1 - \varepsilon) \mathbb{E}[|X - s| | Y - t|] + (1 - \varepsilon)\varepsilon \mathbb{E}[|s - X'| | t - Y'] \\ &= (1 - \varepsilon)^2 \mathbb{E}[|X - X'| | Y - Y'] + 2\varepsilon(1 - \varepsilon) \mathbb{E}[|X - s| | Y - t|]. \end{aligned}$$

The second term yields:

$$\begin{aligned} \mathbb{E}[|X_\varepsilon - X'_\varepsilon|] \mathbb{E}[|Y_\varepsilon - Y'_\varepsilon|] &= \left( (1 - \varepsilon)^2 \mathbb{E}[|X - X'|] + 2\varepsilon(1 - \varepsilon) \mathbb{E}[|X - s|] \right) \\ &\quad \left( (1 - \varepsilon)^2 \mathbb{E}[|Y - Y'|] + 2\varepsilon(1 - \varepsilon) \mathbb{E}[|Y - t|] \right), \end{aligned}$$

as a consequence of

$$\begin{aligned} \mathbb{E}[|X_\varepsilon - X'_\varepsilon|] &= \int |x - x'| f_X^\varepsilon(x) f_X^\varepsilon(x') dx dx' \\ &= (1 - \varepsilon)^2 \mathbb{E}[|X - X'|] + \varepsilon^2 (|s - s|) + (1 - \varepsilon)\varepsilon \mathbb{E}[|X - s|] + \varepsilon(1 - \varepsilon) \mathbb{E}[|s - X'|] \\ &= (1 - \varepsilon)^2 \mathbb{E}[|X - X'|] + 2\varepsilon(1 - \varepsilon) \mathbb{E}[|X - s|]. \end{aligned}$$

Finally, for the third term we obtain

$$\begin{aligned}
& \mathbb{E}[|X_\varepsilon - X'_\varepsilon| |Y_\varepsilon - Y''_\varepsilon|] \\
&= \int |x - x'| |y - y''| f_{X|Y}^\varepsilon(x, y) f_{X'}^\varepsilon(x') f_{Y'}^\varepsilon(y'') dx dx' dy dy'' \\
&= (1 - \varepsilon)^3 \mathbb{E}[|X - X'| |Y - Y''|] \\
&\quad + \varepsilon(1 - \varepsilon)^2 (\mathbb{E}[|s - X'| |t - Y''|] + \mathbb{E}[|X - s| |Y - Y''|] + \mathbb{E}[|X - X'| |Y - t|]) \\
&\quad + \varepsilon^2(1 - \varepsilon) (\mathbb{E}[|s - s| |t - Y''|] + \mathbb{E}[|s - X'| |t - t|] + \mathbb{E}[|X - s| |Y - t|]) + \varepsilon^3(|s - s| |t - t|) \\
&= (1 - \varepsilon)^3 \mathbb{E}[|X - X'| |Y - Y''|] \\
&\quad + \varepsilon(1 - \varepsilon)^2 (\mathbb{E}[|s - X'| |t - Y''|] + \mathbb{E}[|X - s| |Y - Y''|] + \mathbb{E}[|X - X'| |Y - t|]) \\
&\quad + \varepsilon^2(1 - \varepsilon) \mathbb{E}[|X - s| |Y - t|] .
\end{aligned}$$

Putting everything together, we obtain:

$$\begin{aligned}
d\text{Cov}(X_\varepsilon, Y_\varepsilon) &= (\text{term 1}) + (\text{term 2}) - 2^*(\text{term 3}) \\
&= (1 - \varepsilon)^2 \mathbb{E}[|X - X'| |Y - Y''|] + (1 - \varepsilon)^4 \mathbb{E}[|X - X'|] \mathbb{E}[|Y - Y''|] \\
&\quad - 2(1 - \varepsilon)^3 \mathbb{E}[|X - X'| |Y - Y''|] + 2\varepsilon(1 - \varepsilon)^2 \mathbb{E}[|X - s| |Y - t|] \\
&\quad + 2\varepsilon(1 - \varepsilon)^3 \mathbb{E}[|X - s|] \mathbb{E}[|Y - Y''|] + 2\varepsilon(1 - \varepsilon)^3 \mathbb{E}[|X - X'|] \mathbb{E}[|Y - t|] \\
&\quad + 2\varepsilon(1 - \varepsilon)^2 (2\varepsilon - 1) \mathbb{E}[|X - s|] \mathbb{E}[|Y - t|] - 2\varepsilon(1 - \varepsilon)^2 \mathbb{E}[|X - s| |Y - Y''|] \\
&\quad - 2\varepsilon(1 - \varepsilon)^2 \mathbb{E}[|X - X'| |Y - t|] .
\end{aligned}$$

This implies that

$$\text{IF}((s, t), d\text{Cov}, F) = \lim_{\varepsilon \rightarrow 0} \frac{d\text{Cov}(X_\varepsilon, Y_\varepsilon) - d\text{Cov}(X, Y)}{\varepsilon} = \lim_{\varepsilon \rightarrow 0} \frac{a\varepsilon^0 + b\varepsilon^1 + O(\varepsilon^2)}{\varepsilon},$$

where  $a = 0$  and

$$\begin{aligned}
b &= -2\mathbb{E}[|X - X'| |Y - Y''|] - 4\mathbb{E}[|X - X'|] \mathbb{E}[|Y - Y''|] + 6\mathbb{E}[|X - X'| |Y - Y''|] \\
&\quad + 2\mathbb{E}[|X - s| |Y - t|] + 2\mathbb{E}[|X - s|] \mathbb{E}[|Y - Y''|] + 2\mathbb{E}[|X - X'|] \mathbb{E}[|Y - t|] \\
&\quad - 2\mathbb{E}[|X - s|] \mathbb{E}[|Y - t|] - 2\mathbb{E}[|X - s| |Y - Y''|] - 2\mathbb{E}[|X - X'| |Y - t|] .
\end{aligned}$$

Hence we obtain that  $\text{IF}((s, t), \text{dCov}, F) = b$ . This can be further simplified as:

$$\begin{aligned}
b &= -2\mathbb{E}[|X - X'| | Y - Y'|] - 4\mathbb{E}[|X - X'|] \mathbb{E}[|Y - Y'|] + 6\mathbb{E}[|X - X'| | Y - Y''] \\
&\quad + 2\mathbb{E}[|X - s| | Y - t] + 2\mathbb{E}[|X - s|] \mathbb{E}[|Y - Y'|] + 2\mathbb{E}[|X - X'|] \mathbb{E}[|Y - t|] \\
&\quad - 2\mathbb{E}[|X - s|] \mathbb{E}[|Y - t|] - 2\mathbb{E}[|X - s| | Y - Y'] - 2\mathbb{E}[|X - X'| | Y - t] \\
&= -2\text{dCov}(X, Y) - 2\mathbb{E}[|X - X'|] \mathbb{E}[|Y - Y'|] + 2\mathbb{E}[|X - X'| | Y - Y''] \\
&\quad + 2\mathbb{E}[|X - s| | Y - t] + 2\mathbb{E}[|X - s|] \mathbb{E}[|Y - Y'|] + 2\mathbb{E}[|X - X'|] \mathbb{E}[|Y - t|] \\
&\quad - 2\mathbb{E}[|X - s|] \mathbb{E}[|Y - t|] - 2\mathbb{E}[|X - s| | Y - Y'] - 2\mathbb{E}[|X - X'| | Y - t] \\
&= -2\text{dCov}(X, Y) - 2(\mathbb{E}[|X - s|] - \mathbb{E}[|X - X'|])(\mathbb{E}[|Y - t|] - \mathbb{E}[|Y - Y'']]) \\
&\quad + 2\mathbb{E}[(|X - s| - |X - X'|)(|Y - t| - |Y - Y''])] \\
&= -2\text{dCov}(X, Y) + 2\text{Cov}(|X - s| - |X - X'|, |Y - t| - |Y - Y'']) .
\end{aligned}$$

**Proof of Proposition 2** For the (un)boundedness of the IF, we study the behavior of

$$\begin{aligned}
&\text{Cov}(|X - s|^\alpha - |X - X'|^\alpha, |Y - t|^\alpha - |Y - Y''|^\alpha) \\
&= \text{Cov}(|X - s|^\alpha, |Y - t|^\alpha) - \text{Cov}(|X - s|^\alpha, |Y - Y''|^\alpha) \\
&\quad - \text{Cov}(|X - X'|^\alpha, |Y - t|^\alpha) + \text{Cov}(|X - X'|^\alpha, |Y - Y''|^\alpha) .
\end{aligned}$$

Hence we are interested in the first 3 terms. We start with  $\alpha \leq 1$  using Cauchy-Schwarz:

$$\begin{aligned}
|\text{Cov}(|X - s|^\alpha, |Y - t|^\alpha)| &\leq \sqrt{\text{Var}(|X - s|^\alpha) \text{Var}(|Y - t|^\alpha)} \\
|\text{Cov}(|X - s|^\alpha, |Y - Y''|^\alpha)| &\leq \sqrt{\text{Var}(|X - s|^\alpha) \text{Var}(|Y - Y''|^\alpha)} \\
|\text{Cov}(|X - X'|^\alpha, |Y - t|^\alpha)| &\leq \sqrt{\text{Var}(|X - X'|^\alpha) \text{Var}(|Y - t|^\alpha)} .
\end{aligned}$$

Next we show that  $\text{Var}(|X - s|^\alpha)$  and  $\text{Var}(|Y - t|^\alpha)$  are bounded for  $\alpha \leq 1$ :

$$\begin{aligned}
2\text{Var}[|X - s|^\alpha] &= \mathbb{E}[(|X - s|^\alpha - |X' - s|^\alpha)^2] \\
&\leq \mathbb{E}[(|X - X'|^{2\alpha})] \\
&\leq 1 + \mathbb{E}[|X - X'|^2] \\
&= 1 + 2\text{Var}[X] .
\end{aligned}$$

Here the first inequality holds because it holds for any  $(x, x')$  when  $0 \leq \alpha \leq 1$ . As the last quantity does not depend on  $s$ , this yields an upper bound and hence the  $\alpha$ -distance covariance has a bounded IF for  $\alpha \leq 1$ . For  $\alpha < 1$  the variance (and covariances) of interest are even redescending, see the proof of Proposition 3.

Second we discuss  $\alpha > 1$ . The unboundedness of  $\text{Cov}(|X - s|^\alpha, |Y - t|^\alpha)$  depends on the dependence between  $X$  and  $Y$ . For example, if  $X$  and  $Y$  are independent, then  $|X - s|^\alpha$  and  $|Y - t|^\alpha$  are also independent and the term equals zero, just as the other two terms. However, when  $X = Y$  and  $t = s$ , we obtain the IF of  $\alpha$ -distance variance which we show to be unbounded for  $\alpha > 1$  in the proof of Proposition 3.

## A.2 | Proofs of Section 2.2

**Proof of Corollary 1** For the first statement we use

$$\begin{aligned} \text{IF}(s, \text{dVar}(X; \alpha), F_X) &= \text{IF}((s, s), \text{dCov}(X, X; \alpha), F_X) \\ &= -2\text{dVar}(X; \alpha) + 2\eta(s, s, X, X, \alpha). \end{aligned}$$

For the second statement we compute

$$\begin{aligned} \text{IF}(s, \text{dVar}(X; \alpha), F_X) &= \frac{\partial}{\partial \varepsilon} (\text{dVar}(X_\varepsilon; \alpha)) \Big|_{\varepsilon=0} \\ &= \frac{\partial}{\partial \varepsilon} (\text{dStd}(X_\varepsilon; \alpha)^2) \Big|_{\varepsilon=0} \\ &= 2\text{dStd}(X; \alpha) \frac{\partial}{\partial \varepsilon} (\text{dStd}(X_\varepsilon; \alpha)) \Big|_{\varepsilon=0} \\ &= 2\text{dStd}(X; \alpha) \text{IF}(s, \text{dStd}(X; \alpha), F). \end{aligned}$$

**Proof of Proposition 3** To investigate the boundedness of the IF of the  $\alpha$ -distance variance, we study the behavior of

$$\text{Var}[|X - s|^\alpha] - 2\text{Cov}[|X - s|^\alpha, |X - X'|^\alpha].$$

For  $\alpha \leq 1$ , we have already proven the boundedness of these terms in the proof of Proposition 2.

Next, we consider  $\alpha > 1$ . For the variance term, we assume that  $X$  is not degenerate, so there exists an  $\varepsilon > 0$  such that the probability  $p := \Pr(|X - X'| \geq \varepsilon)$  is strictly positive. Also denote  $A_\varepsilon = \{(X - s)(X' - s) > 0\}$ , i.e. the event that  $(X - s)$  and  $(X' - s)$  have the same sign. Clearly,  $\lim_{s \rightarrow \infty} \Pr(A_\varepsilon) = 1$ . We now have

$$\begin{aligned} 2\text{Var}[|X - s|^\alpha] &= \mathbb{E}[ (|X - s|^\alpha - |X' - s|^\alpha)^2 ] \\ &\geq \mathbb{E}[ (|X - s|^\alpha - |X' - s|^\alpha)^2 \mid |X - X'| \geq \varepsilon ] \Pr(|X - X'| \geq \varepsilon) \\ &= p \mathbb{E}[ (|X - s|^\alpha - |X' - s|^\alpha)^2 \mid |X - X'| \geq \varepsilon ] \\ &\geq p \mathbb{E}[ (|X - s|^\alpha - |X' - s|^\alpha)^2 \mid |X - X'| \geq \varepsilon \cap A_\varepsilon ] \Pr(A_\varepsilon) \\ &\geq p\alpha^2 \mathbb{E}[ \min\{|X - s|, |X' - s|\}^{2(\alpha-1)} |X - X'|^2 \mid |X - X'| \geq \varepsilon \cap A_\varepsilon ] \Pr(A_\varepsilon) \\ &\geq p\alpha^2 \varepsilon^2 \mathbb{E}[ \min\{|X - s|, |X' - s|\}^{2(\alpha-1)} \mid |X - X'| \geq \varepsilon \cap A_\varepsilon ] \Pr(A_\varepsilon), \end{aligned}$$

where we have used the convexity of  $x \rightarrow x^\alpha$  for  $\alpha > 1$  in the second inequality (i.e. the graph lies above its tangents). The last term blows up as  $s \rightarrow \infty$ , because  $2(\alpha - 1) > 0$  and  $\lim_{s \rightarrow \infty} \Pr(A_\varepsilon) = 1$ . We thus obtain that  $\text{Var}[|X - s|^\alpha]$  is unbounded.

This gives us

$$\begin{aligned} &\text{Var}[|X - s|^\alpha] - 2\text{Cov}[|X - s|^\alpha, |X - X'|^\alpha] \\ &\geq \text{Var}[|X - s|^\alpha] - 2|\text{Cov}[|X - s|^\alpha, |X - X'|^\alpha]| \\ &\geq \text{Var}[|X - s|^\alpha] - 2\sqrt{\text{Var}[|X - s|^\alpha]\text{Var}[|X - X'|^\alpha]} \\ &= \text{Var}[|X - s|^\alpha] - 2C\sqrt{\text{Var}[|X - s|^\alpha]}, \end{aligned}$$

by using Cauchy-Schwarz. This explodes because  $\text{Var}[|X - s|^\alpha]$  explodes for  $s \rightarrow \infty$  when  $\alpha > 1$ . Therefore  $\text{Var}[|X - s|^\alpha] - 2\text{Cov}[|X - s|^\alpha, |X - X'|^\alpha]$  is unbounded for  $\alpha > 1$ .

Lastly, we consider  $2\text{Var}[|X - s|^\alpha] = \mathbb{E}[ (|X - s|^\alpha - |X' - s|^\alpha)^2 ]$  with  $\alpha < 1$ . Note that, due to the concavity of  $x \rightarrow x^\alpha$  for  $\alpha < 1$ , we have

$$||X - s|^\alpha - |X' - s|^\alpha| \leq \alpha \min\{|s - X|, |s - X'|\}^{\alpha-1} |X - X'|.$$

Unlike in the previous case for  $\alpha > 1$ , we do not need to consider  $A_s$  here, since the above is true even if  $(s - X)$  and  $(s - X')$  have a different sign.

$$\begin{aligned} 2\text{Var}[|X - s|^\alpha] &= \mathbb{E}[(|X - s|^\alpha - |X' - s|^\alpha)^2] \\ &\leq \alpha^2 \mathbb{E}[\min\{|s - X|, |s - X'|\}^{2(\alpha-1)} |X - X'|^2] \end{aligned}$$

given that  $2(\alpha - 1) < 0$  and  $\mathbb{E}[|X - X'|^2] < \infty$ , this converges to 0. Therefore  $\text{Var}[|X - s|^\alpha]$  converges to 0 for  $s \rightarrow \infty$  if  $\alpha < 1$ .

### A.3 | Proofs of Section 2.3

**Proof of Corollary 2** We omit  $\alpha$  to ease the notational burden, but the computation is the same. We compute

$$\begin{aligned}
\text{IF}((s, t), \text{dCor}, F) &= \frac{\partial}{\partial \varepsilon} \left( \frac{\text{dCov}(X_\varepsilon, Y_\varepsilon)}{\sqrt{\text{dVar}(X_\varepsilon)\text{dVar}(Y_\varepsilon)}} \right) \Bigg|_{\varepsilon=0} \\
&= \left[ \text{IF}(\text{dCov}(X, Y))\sqrt{\text{dVar}(X)\text{dVar}(Y)} - \frac{1}{2\sqrt{\text{dVar}(X)\text{dVar}(Y)}} (\text{IF}(\text{dVar}(X))\text{dVar}(Y) \right. \\
&\quad \left. + \text{dVar}(X)\text{IF}(\text{dVar}(Y)))\text{dCov}(X, Y) \right] / (\text{dVar}(X)\text{dVar}(Y)) \\
&= \frac{\text{IF}(\text{dCov}(X, Y))}{\text{dStd}(X)\text{dStd}(Y)} - \frac{\text{IF}(\text{dVar}(X))\text{dVar}(Y) + \text{dVar}(X)\text{IF}(\text{dVar}(Y))}{2(\text{dVar}(X)\text{dVar}(Y))} \frac{\text{dCov}(X, Y)}{\sqrt{\text{dVar}(X)\text{dVar}(Y)}} \\
&= \frac{\text{IF}(\text{dCov}(X, Y))}{\text{dStd}(X)\text{dStd}(Y)} - \left( \frac{\text{IF}(\text{dVar}(X))}{2\text{dVar}(X)} + \frac{\text{IF}(\text{dVar}(Y))}{2\text{dVar}(Y)} \right) \text{dCor}(X, Y) \\
&= \frac{-2\text{dCov}(X, Y) + 2\text{Cov}(|X - s| - |X - X'|, |Y - t| - |Y - Y''|)}{\text{dStd}(X)\text{dStd}(Y)} \\
&\quad - \left( \frac{-2\text{dVar}(X) + 2\text{Cov}(|X - s| - |X - X'|, |X - s| - |X - X''|)}{2\text{dVar}(X)} \right. \\
&\quad \left. + \frac{-2\text{dVar}(Y) + 2\text{Cov}(|Y - t| - |Y - Y'|, |Y - t| - |Y - Y''|)}{2\text{dVar}(Y)} \right) \text{dCor}(X, Y) \\
&= -2\text{dCor}(X, Y) + \frac{2\text{Cov}(|X - s| - |X - X'|, |Y - t| - |Y - Y''|)}{\text{dStd}(X)\text{dStd}(Y)} - \\
&\quad \left( -2 + \frac{\text{Cov}(|X - s| - |X - X'|, |X - s| - |X - X''|)}{\text{dVar}(X)} \right. \\
&\quad \left. + \frac{\text{Cov}(|Y - t| - |Y - Y'|, |Y - t| - |Y - Y''|)}{\text{dVar}(Y)} \right) \text{dCor}(X, Y) \\
&= \frac{2\text{Cov}(|X - s| - |X - X'|, |Y - t| - |Y - Y''|)}{\text{dStd}(X)\text{dStd}(Y)} \\
&\quad - \left( \frac{\text{Cov}(|X - s| - |X - X'|, |X - s| - |X - X''|)}{\text{dVar}(X)} \right. \\
&\quad \left. + \frac{\text{Cov}(|Y - t| - |Y - Y'|, |Y - t| - |Y - Y''|)}{\text{dVar}(Y)} \right) \text{dCor}(X, Y).
\end{aligned}$$

**Proof of Proposition 4** For the IF of the  $\alpha$ -distance correlation we had the following expression:

$$\frac{2\eta(s, t, X, Y, \alpha)}{dStd(X; \alpha)dStd(Y; \alpha)} - \left( \frac{\eta(s, s, X, X, \alpha)}{dVar(X; \alpha)} + \frac{\eta(t, t, Y, Y, \alpha)}{dVar(Y; \alpha)} \right) dCor(X, Y; \alpha).$$

As shown in its derivation, this can also be written as

$$\frac{IF(dCov(X, Y; \alpha))}{dStd(X; \alpha)dStd(Y; \alpha)} - \left( \frac{IF(dVar(X; \alpha))}{2dVar(X; \alpha)} + \frac{IF(dVar(Y; \alpha))}{2dVar(Y; \alpha)} \right) dCor(X, Y; \alpha).$$

Hence we immediately have that the IF of  $dCor(X, Y; \alpha)$  is bounded (and redescending) for  $\alpha \leq 1$  ( $\alpha < 1$ ) as it is a combination of bounded (and redescending) terms. For  $\alpha > 1$ , the (un)boundedness of the IF again depends on the distribution of  $(X, Y)$ .

## B | DISTANCE STANDARD DEVIATION AS A SCALE ESTIMATOR

In this part of the Supplementary Material, we undertake a more detailed analysis of the distance standard deviation as a scale estimator. More precisely, we study its theoretical efficiency and perform a small simulation to assess its robustness.

First, we calculate its asymptotic variance (ASV) to derive its efficiency (eff). For this, we study the consistent estimator  $\sqrt{v_\alpha} \bar{c} \text{dStd}(X; \alpha)^{1/\alpha}$  at the normal model  $\mathcal{N}(0, \sigma^2)$ .

$$\begin{aligned}
 \text{IF}(s, \sqrt{v_\alpha} \bar{c} \text{dStd}(X; \alpha)^{1/\alpha}, \Phi) &= \frac{\partial}{\partial \varepsilon} \left( \sqrt{v_\alpha} \bar{c} \text{dStd}(X_\varepsilon; \alpha)^{1/\alpha} \right) \Big|_{\varepsilon=0} \\
 &= \sqrt{v_\alpha} \bar{c} \frac{1}{\alpha} (\text{dStd}(X; \alpha))^{\frac{1}{\alpha}-1} \frac{\partial}{\partial \varepsilon} (\text{dStd}(X_\varepsilon; \alpha)) \Big|_{\varepsilon=0} \\
 &= \frac{1}{\alpha} (\text{dStd}(X; \alpha))^{-1} \text{IF}(s, \text{dStd}(X; \alpha), \Phi) \\
 &= \frac{(\text{dStd}(X; \alpha))^{-1} \text{IF}(s, \text{dVar}(X; \alpha), \Phi)}{\alpha \frac{2 \text{dStd}(X; \alpha)}{2 \text{dStd}(X; \alpha)}} \\
 &= \frac{\text{IF}(s, \text{dVar}(X; \alpha), \Phi)}{2\alpha \text{dVar}(X; \alpha)}
 \end{aligned}$$

$$\Rightarrow \text{ASV}(\sqrt{v_\alpha} \bar{c} \text{dStd}(X; \alpha)^{1/\alpha}, \Phi) = \mathbb{E}_\Phi[\text{IF}(s, \sqrt{v_\alpha} \bar{c} \text{dStd}(X; \alpha)^{1/\alpha}, \Phi)^2]$$

$$\Rightarrow \text{eff}(\sqrt{v_\alpha} \bar{c} \text{dStd}(X; \alpha)^{1/\alpha}, \Phi) = \frac{1}{2 \text{ASV}(\sqrt{v_\alpha} \bar{c} \text{dStd}(X; \alpha)^{1/\alpha}, \Phi)}$$

where 2 is the Fisher information of  $\sigma$  at the scale model  $\mathcal{N}(0, \sigma^2)$ . Calculating the integrals numerically in Mathematica we obtain the following efficiencies per  $\alpha$ :

$\alpha$	0.6	0.7	0.8	0.9	1	1.1	1.2	1.3	1.4
efficiency	0.5793	0.6380	0.6911	0.7396	0.7839	0.8244	0.8610	0.8936	0.9220

Naturally, the efficiency increases towards 1 when  $\alpha \rightarrow 2$  because then the estimate converges to the classical standard deviation. To study the finite-sample efficiency of  $\sqrt{v_\alpha} \bar{c} \text{dStd}(X; \alpha)$ , we compare it to scale M-estimators with the same influence function per  $\alpha$ .

In Figure 22 the M-estimators converge faster to the theoretical efficiencies than the  $\alpha$ -distance standard deviation, but both estimators converge rather fast. The convergence is also faster for higher  $\alpha$ , when the estimator gets closer to the classical standard deviation.

Next, we compare the robustness of  $\sqrt{v_\alpha} \bar{c} \text{dStd}(X; \alpha)^{1/\alpha}$  per  $\alpha$  with the robustness of the corresponding M-estimators and the classical standard deviation. We do this for the following 4 standard normal settings containing 100% contamination:

1.  $(1 - \varepsilon) \mathcal{N}(0, 1) + \varepsilon \mathcal{N}(3, 1)$
2.  $(1 - \varepsilon) \mathcal{N}(0, 1) + \varepsilon \mathcal{N}(6, 1)$
3.  $(1 - \varepsilon) \mathcal{N}(0, 1) + \varepsilon \mathcal{N}(0, 4)$
4.  $\mathcal{N}(0, 1)$  with one outlier added in  $x$ .

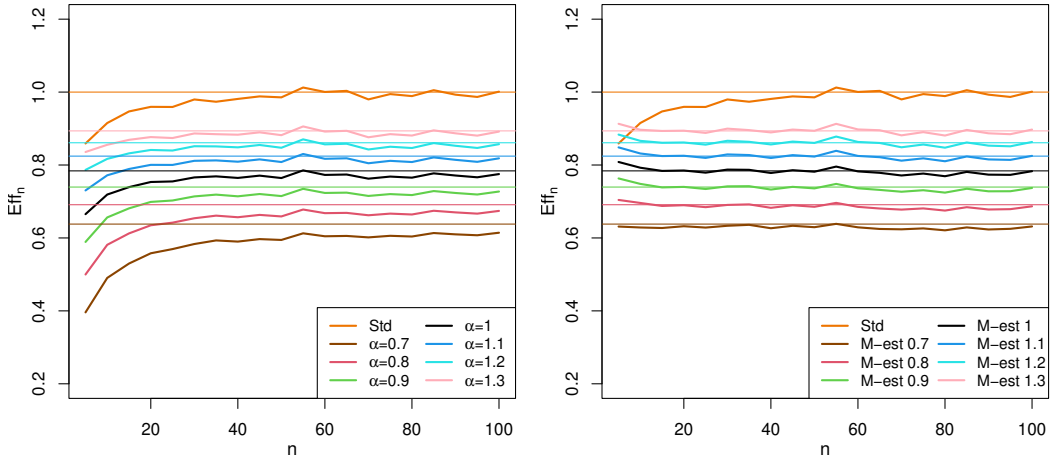
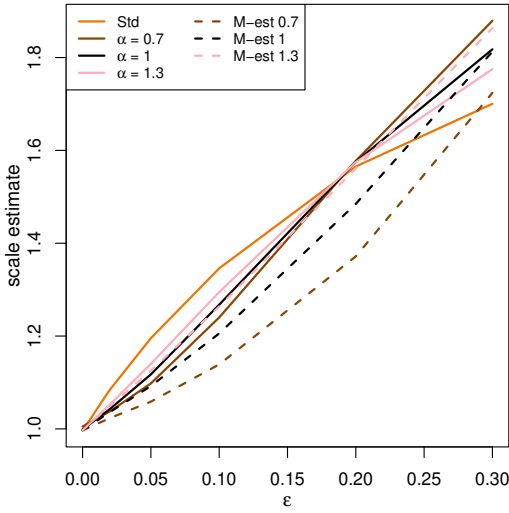


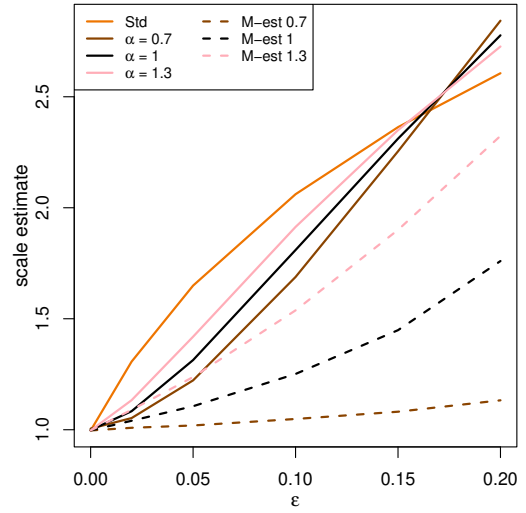
**FIGURE 22** Finite-sample efficiencies for different sample sizes for: on the left the consistent  $\alpha$ -distance standard deviation for different  $\alpha$ , and on the right the scale M-estimators with the same influence functions as the estimators in the left figure.

In each setting we draw 1000 samples of size  $n = 300$  and compute the scale estimators. Their average values are shown in Figure 23.

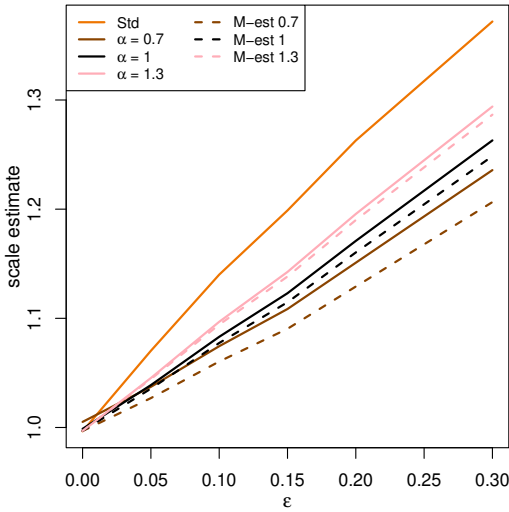
In these graphs the contamination affects every scale estimator. Among them, the M-estimator with  $\alpha = 0.7$  appears to be the most resistant. While the  $\alpha$ -distance standard deviations are less robust, they are still superior to the classical measure. We also observe that the  $\alpha$ -distance standard deviation is more robust for low  $\alpha$  values, which is in agreement with the influence functions in the main text.



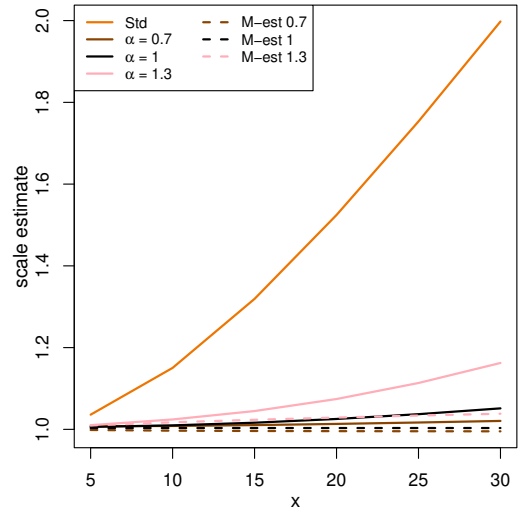
(1) contaminated by  $\mathcal{N}(3, 1)$ .



(2) contaminated by  $\mathcal{N}(6, 1)$ .



(3) contaminated by  $\mathcal{N}(0, 4)$ .



(4) contaminated by one outlier in  $x$ .

**FIGURE 23** Average value of the  $\alpha$ -distance standard deviation, the corresponding M-estimator, and the classical standard deviation, in the 4 settings.

## C | PROOFS OF THE BREAKDOWN VALUES IN SECTION 3

### C.1 | Finite-sample breakdown values

From the expression

$$d_{1j} = |s - x_j|^\alpha = u^2 + O(u)$$

we derive

$$\overline{d_{1.}} = \frac{1}{n} \sum_{j \neq 1} (u^2 + O(u)) = \frac{n-1}{n} u^2 + O(u) .$$

For  $i \neq 1$  we obtain

$$\overline{d_{i.}} = \frac{1}{n} \sum_{j=1}^n d_{ij} = \frac{1}{n} \left( d_{i1} + \sum_{j=2}^n d_{ij} \right) = \frac{1}{n} (u^2 + O(u) + o(u)) = \frac{u^2}{n} + O(u)$$

and for  $j \neq 1$  it holds by symmetry that

$$\overline{d_{.j}} = \frac{u^2}{n} + O(u) .$$

Finally

$$\begin{aligned} \overline{d_{..}} &= \frac{1}{n} \sum_{i=1}^n \overline{d_{i.}} = \frac{1}{n} \left( \overline{d_{1.}} + \sum_{i=2}^n \overline{d_{i.}} \right) \\ &= \frac{1}{n} \left( \frac{n-1}{n} u^2 + O(u) + (n-1) \left( \frac{u^2}{n} + O(u) \right) \right) = \frac{2(n-1)}{n^2} u^2 + O(u) . \end{aligned}$$

Next we find for all  $j \neq 1$  that

$$\begin{aligned} \Delta_{1j} &= d_{1j} - \overline{d_{1.}} - \overline{d_{.j}} + \overline{d_{..}} \\ &= u^2 - \frac{n-1}{n} u^2 - \frac{1}{n} u^2 + \frac{2(n-1)}{n^2} u^2 + O(u) \\ &= \frac{2(n-1)}{n^2} u^2 + O(u) \end{aligned}$$

and

$$\begin{aligned} \Delta_{11} &= d_{11} - \overline{d_{1.}} - \overline{d_{.1}} + \overline{d_{..}} \\ &= 0 - \frac{n-1}{n} u^2 - \frac{n-1}{n} u^2 + \frac{2(n-1)}{n^2} u^2 + O(u) \\ &= \frac{-2(n-1)}{n} u^2 + \frac{2(n-1)}{n^2} u^2 + O(u) \\ &= \frac{-2(n-1)^2}{n^2} u^2 + O(u) . \end{aligned}$$

For the remaining  $(i, j)$  with  $i \neq 1 \neq j$  we find

$$\Delta_{ij} = -\frac{1}{n}u^2 - \frac{1}{n}u^2 + \frac{2(n-1)}{n^2}u^2 + O(u) = \frac{-2}{n^2}u^2 + O(u).$$

The overall distance variance of the dataset  $X$  then yields

$$\begin{aligned} d\text{Var}(X) &= \frac{1}{n^2} \sum_{i,j=1}^n \Delta_{ij}^2 \\ &= \frac{1}{n^2} \left[ \Delta_{11}^2 + \sum_{j=2}^n \Delta_{1j}^2 + \sum_{i=2}^n \Delta_{i1}^2 + \sum_{i,j=2}^n \Delta_{ij}^2 \right] \\ &= \frac{1}{n^2} \left[ \left( \frac{-2(n-1)^2}{n^2} u^2 \right)^2 + 2(n-1) \left( \frac{2(n-1)^2}{n^2} u^2 \right)^2 + (n-1)^2 \left( \frac{-2}{n^2} u^2 \right)^2 + n^2 O(u^3) \right] \\ &= \frac{4}{n^6} u^4 [(n-1)^4 + 2(n-1)^3 + (n-1)^2] + O(u^3) \\ &= 4 \frac{(n-1)^2}{n^4} u^4 + O(u^3). \end{aligned}$$

For the finite-sample breakdown value of  $d\text{Cov}$  we obtain analogously

$$\begin{aligned} d\text{Cov}(Z) &= \frac{1}{n^2} \sum_{i,j=1}^n \Delta_{X,i,j} \Delta_{Y,i,j} \\ &= \frac{1}{n^2} \left[ \Delta_{X,1,1} \Delta_{Y,1,1} + \sum_{j=2}^n \Delta_{X,1,j} \Delta_{Y,1,j} + \sum_{i=2}^n \Delta_{X,i,1} \Delta_{Y,i,1} + \sum_{i,j=2}^n \Delta_{X,i,j} \Delta_{Y,i,j} \right] \\ &= \dots = 4 \frac{(n-1)^2}{n^4} s^\alpha t^\alpha + O(s^{3\alpha/4} t^{3\alpha/4}) \\ &\approx \frac{4}{n^2} s^\alpha t^\alpha + O(s^{3\alpha/4} t^{3\alpha/4}). \end{aligned}$$

## C.2 | Asymptotic breakdown value of $d\text{Var}$

Take  $H = \Delta_s$  and consider  $F_\varepsilon = (1 - \varepsilon)F + \varepsilon H$ . Then the three terms of the distance variance become

$$E[\|X_\varepsilon - X'_\varepsilon\|^2] = (1 - \varepsilon)^2 E[\|X - X'\|^2] + 2\varepsilon(1 - \varepsilon) E[\|X - s\|^2],$$

$$E[\|X_\varepsilon - X''_\varepsilon\|^2] = ((1 - \varepsilon)^2 E[\|X - X'\|] + 2\varepsilon(1 - \varepsilon) E[\|X - s\|])^2,$$

$$\begin{aligned} E[\|X_\varepsilon - X'_\varepsilon\| \|X_\varepsilon - X''_\varepsilon\|] &= (1 - \varepsilon)^3 E[\|X - X'\| \|X - X''\|] \\ &\quad + 2\varepsilon(1 - \varepsilon)^2 E[\|X - X'\| \|X - s\|] \\ &\quad + \varepsilon(1 - \varepsilon)^2 E[\|s - X'\| \|s - X''\|] \\ &\quad + \varepsilon^2(1 - \varepsilon) E[\|X - s\|^2]. \end{aligned}$$

If we reconstruct  $d\text{Var}$  from these terms (summing the first two and subtracting twice the third term), we obtain

$$\begin{aligned} d\text{Var}(F, \varepsilon, s) &= \text{constant} \\ &+ \left\{ 2\varepsilon(1 - \varepsilon) - 2\varepsilon^2(1 - \varepsilon) \right\} E[||X - s||^2] \\ &+ \left\{ 4\varepsilon^2(1 - \varepsilon)^2 - 2(1 - \varepsilon)^2\varepsilon \right\} E[||X - s||]^2 \\ &+ 4\varepsilon(1 - \varepsilon)^3 E[||X - X' ||] E[||X - s ||] \\ &- 4\varepsilon(1 - \varepsilon)^2 E[||X - X' || ||X - s ||] . \end{aligned}$$

This can be simplified to

$$\begin{aligned} d\text{Var}(F, \varepsilon, s) &= 2\varepsilon(1 - \varepsilon)^2 E[||X - s||^2] \\ &+ 2\varepsilon(1 - \varepsilon)^2(2\varepsilon - 1) E[||X - s||]^2 \\ &+ 4\varepsilon(1 - \varepsilon)^3 E[||X - X' ||] E[||X - s ||] \\ &- 4\varepsilon(1 - \varepsilon)^2 E[||X - X' || ||X - s ||] \\ &+ \text{constant} . \end{aligned}$$

Note that the second term is negative. Now note that for the first and second term, we can bound them (using the fact that the variance is non-negative) from below by

$$\begin{aligned} &2\varepsilon(1 - \varepsilon)^2 E[||X - s||^2] + 2\varepsilon(1 - \varepsilon)^2(2\varepsilon - 1) E[||X - s||]^2 \\ &\geq 2\varepsilon(1 - \varepsilon)^2 E[||X - s||^2] + 2\varepsilon(1 - \varepsilon)^2(2\varepsilon - 1) E[||X - s||]^2 \\ &= 4\varepsilon^2(1 - \varepsilon)^2 E[||X - s||^2] . \end{aligned}$$

Dropping the positive third term, we obtain :

$$\begin{aligned} d\text{Var}(F, \varepsilon, s) &\geq \text{constant} \\ &+ 4\varepsilon^2(1 - \varepsilon)^2 E[||X - s||^2] \\ &- 4\varepsilon(1 - \varepsilon)^2 E[||X - X' || ||X - s ||] \\ &\geq \text{constant} \\ &+ 4\varepsilon^2(1 - \varepsilon)^2 E[||X - s||^2] \\ &- 4\varepsilon(1 - \varepsilon)^2 \sqrt{E[||X - X' ||^2] E[||X - s ||^2]} \\ &\geq \text{constant} \\ &+ \left\{ 2\varepsilon(1 - \varepsilon) \sqrt{E[||X - s ||^2]} - (1 - \varepsilon) \sqrt{E[||X - X' ||^2]} \right\}^2 \\ &- (1 - \varepsilon)^2 E[||X - X' ||^2] \\ &\geq \text{constant}' \\ &+ \left\{ 2\varepsilon(1 - \varepsilon) \sqrt{E[||X - s ||^2]} - (1 - \varepsilon) \sqrt{E[||X - X' ||^2]} \right\}^2 , \end{aligned}$$

where we have used Cauchy-Schwarz for the second inequality and completed the square for the second-to-last equality. For any fixed  $\varepsilon$ , the last term explodes as  $s$  goes to  $\infty$ .

### C.3 | Asymptotic breakdown value of dCov

Take  $H = \Delta_{(s,s)}$  and consider  $F_\varepsilon = (1 - \varepsilon)F + \varepsilon H$ . We will show that adding a point mass at  $(s, s)$  can make  $\text{dCov}(F_\varepsilon)$  arbitrarily large. The three terms of the distance covariance become

$$E[|X_\varepsilon - X'_\varepsilon| |Y_\varepsilon - Y'_\varepsilon|] = (1 - \varepsilon)^2 E[|X - X'| |Y - Y'|] + 2\varepsilon(1 - \varepsilon) E[|X - s| |Y - s|]$$

$$\begin{aligned} E[|X_\varepsilon - X'_\varepsilon|] E[|Y_\varepsilon - Y'_\varepsilon|] &= (1 - \varepsilon)^4 E[|X - X'|] E[|Y - Y'|] \\ &\quad + 2\varepsilon(1 - \varepsilon)^3 \{E[|X - s|] E[|Y - Y'|] + E[|X - X'|] E[|Y - s|]\} \\ &\quad + 4\varepsilon^2(1 - \varepsilon)^2 E[|X - s|] E[|Y - s|] \end{aligned}$$

$$\begin{aligned} E[|X_\varepsilon - X'_\varepsilon| |Y_\varepsilon - Y''_\varepsilon|] &= (1 - \varepsilon)^3 E[|X - X'| |Y - Y''|] \\ &\quad + \varepsilon(1 - \varepsilon)^2 \{E[|X - X'| |Y - s|] + E[|X - s|] E[|Y - s|]\} \\ &\quad + E[|X - s| |Y - Y''|] \\ &\quad + \varepsilon^2(1 - \varepsilon) E[|X - s| |Y - s|]. \end{aligned}$$

Then we obtain:

$$\begin{aligned} \text{dCov}(F_\varepsilon) &= \text{constant} \\ &\quad + E[|X - s| |Y - s|] \{2\varepsilon(1 - \varepsilon) - 2\varepsilon^2(1 - \varepsilon)\} \\ &\quad + E[|X - s|] E[|Y - s|] \{4\varepsilon^2(1 - \varepsilon)^2 - 2\varepsilon(1 - \varepsilon)^2\} \\ &\quad + E[|X - X'|] E[|Y - s|] \{2\varepsilon(1 - \varepsilon)^3\} \\ &\quad + E[|X - X'| |Y - s|] \{-2(1 - \varepsilon)^2\varepsilon\} \\ &\quad + E[|X - s|] E[|Y - Y'|] \{2\varepsilon(1 - \varepsilon)^3\} \\ &\quad + E[|X - s| |Y - Y'|] \{-2(1 - \varepsilon)^2\varepsilon\}. \end{aligned}$$

Simplifying:

$$\begin{aligned}
d\text{Cov}(F_\varepsilon) &= E[|X - s||Y - s|] \left\{ 2\varepsilon(1 - \varepsilon)^2 \right\} \\
&\quad + E[|X - s|]E[|Y - s|] \left\{ -2\varepsilon(1 - \varepsilon)^2(1 - 2\varepsilon) \right\} \\
&\quad + E[|X - X'|]E[|Y - s|] \left\{ 2\varepsilon(1 - \varepsilon)^3 \right\} \\
&\quad + E[|X - X'||Y - s|] \left\{ -2(1 - \varepsilon)^2\varepsilon \right\} \\
&\quad + E[|X - s|]E[|Y - Y'|] \left\{ 2\varepsilon(1 - \varepsilon)^3 \right\} \\
&\quad + E[|X - s||Y - Y'|] \left\{ -2(1 - \varepsilon)^2\varepsilon \right\} \\
&\quad + \text{constant}.
\end{aligned}$$

Now we need to show that this explodes for  $s \rightarrow \infty$ . Consider the first two terms only, which are the only ones that are "quadratic" in  $s$ . Consider the first term  $E[|X - s||Y - s|]$ . By Cauchy-Schwarz, we have

$$E[|X - s||Y - s|] \geq E[|X - s|]E[|Y - s|] - \sqrt{\text{Var}[|X - s|]\text{Var}[|Y - s|]}.$$

For  $s$  large enough, we have  $\sqrt{\text{Var}[|X - s|]\text{Var}[|Y - s|]} \approx \sqrt{\text{Var}[X]\text{Var}[Y]}$ . Using this, we can lower bound the first two terms (for  $s$  large enough) by:

$$\begin{aligned}
&E[|X - s||Y - s|] \left\{ 2\varepsilon(1 - \varepsilon)^2 \right\} + E[|X - s|]E[|Y - s|] \left\{ -2\varepsilon(1 - \varepsilon)^2(1 - 2\varepsilon) \right\} \\
&\geq 4\varepsilon^2(1 - \varepsilon)^2 E[|X - s||Y - s|] - \left\{ 2\varepsilon(1 - \varepsilon)^2(1 - 2\varepsilon) \right\} \sqrt{\text{Var}[X]\text{Var}[Y]}.
\end{aligned}$$

Therefore we have

$$\begin{aligned}
d\text{Cov}(F_\varepsilon) &\geq \text{constant} \\
&\quad + 4\varepsilon^2(1 - \varepsilon)^2 E[|X - s||Y - s|] \\
&\quad - \left\{ 2\varepsilon(1 - \varepsilon)^2(1 - 2\varepsilon) \right\} \sqrt{\text{Var}[X]\text{Var}[Y]} \\
&\quad + E[|X - X'|]E[|Y - s|] \left\{ 2\varepsilon(1 - \varepsilon)^3 \right\} \\
&\quad + E[|X - X'||Y - s|] \left\{ -2(1 - \varepsilon)^2\varepsilon \right\} \\
&\quad + E[|X - s|]E[|Y - Y'|] \left\{ 2\varepsilon(1 - \varepsilon)^3 \right\} \\
&\quad + E[|X - s||Y - Y'|] \left\{ -2(1 - \varepsilon)^2\varepsilon \right\}.
\end{aligned}$$

We can drop the fourth and sixth terms as they are positive, and absorb the third term in the constant:

$$\begin{aligned} d\text{Cov}(F_\varepsilon) &\geq \text{constant} \\ &+ 4\varepsilon^2(1-\varepsilon)^2 E[|X-s||Y-s|] \\ &+ E[|X-X'||Y-s|] \{-2(1-\varepsilon)^2\varepsilon\} \\ &+ E[|X-s||Y-Y'|] \{-2(1-\varepsilon)^2\varepsilon\}. \end{aligned}$$

It now becomes clearer that we have something quadratic in  $s$ , and some terms which are linear in  $s$ . It suffices to show that the expression

$$\begin{aligned} &2\varepsilon^2(1-\varepsilon)^2 E[|X-s||Y-s|] - 2(1-\varepsilon)^2\varepsilon E[|X-X'||Y-s|] \\ &= 2\varepsilon(1-\varepsilon)^2 E[(\varepsilon|X-s| - |X-X'|) |Y-s|]. \end{aligned}$$

explodes for  $s \rightarrow \infty$ . We can write

$$\begin{aligned} &E[(\varepsilon|X-s| - |X-X'|) |Y-s|] \\ &\geq E[(\varepsilon|s| - \varepsilon|X| - |X| - |X'|) |Y-s|] \\ &= E[\varepsilon|s| |Y-s|] - E[(1+\varepsilon)|X| + |X'|] |Y-s| \\ &\geq \varepsilon E[|s| (|s| - |Y|)] - E[(1+\varepsilon)|X| + |X'|] (|Y| + |s|) \\ &:= a|s|^2 - b|s| - c \end{aligned}$$

for some  $a, b, c > 0$ . This indeed explodes as  $|s| \rightarrow \infty$ .

## D | DISTANCE CORRELATION AFTER RANK TRANSFORMS

**Proposition 5** *The influence function of  $d\text{Cov}(F_X(X), F_Y(Y))$  is given by*

$$\begin{aligned} IF((s, t), d\text{Cov}(F_X(X), F_Y(Y)), F) = & -4d\text{Cov}(F_X(X), F_Y(Y)) \\ & + 2\eta(F_X(s), F_Y(t), F_X(X), F_Y(Y), 1) \\ & + d\text{Cov}(I(X \geq s), F_Y(Y)) \\ & + d\text{Cov}(I(Y \geq t), F_X(X)). \end{aligned}$$

*The IF of  $d\text{Cov}(\Phi^{-1}(F_X(X)), \Phi^{-1}(F_Y(Y)))$  is given by*

$$\begin{aligned} & IF((s, t), d\text{Cov}(\Phi^{-1}(F_X(X)), \Phi^{-1}(F_Y(Y))), F) \\ = & -2d\text{Cov}(X, Y) + 2\eta(s, t, X, Y, 1) \\ & + 2\mathbb{E}\left[\text{sign}(X - X') \left( \frac{I(X \geq s) - \Phi(X)}{\phi(X)} \right) \right. \\ & \quad \left. (|Y - Y'| + \mathbb{E}[|Y - Y'|] - |Y - Y''| - |Y' - Y''|) \right] \\ & + 2\mathbb{E}\left[\text{sign}(Y - Y') \left( \frac{I(Y \geq t) - \Phi(Y)}{\phi(Y)} \right) \right. \\ & \quad \left. (|X - X'| + \mathbb{E}[|X - X'|] - |X - X''| - |X' - X''|) \right] \end{aligned}$$

for bivariate normal  $(X, Y)$ .

From these we can easily derive the corresponding influence functions for the dCor using Corollary 2. The proof of this proposition follows the proof of Proposition 1, but takes into account the dependence of the rank transforms on the contamination.

## E | ADDITIONAL SIMULATION RESULTS

Figure 24 below presents the results of the power simulation for the bivariate settings which were not shown in the main text. The performance differences between the various methods are smaller here.

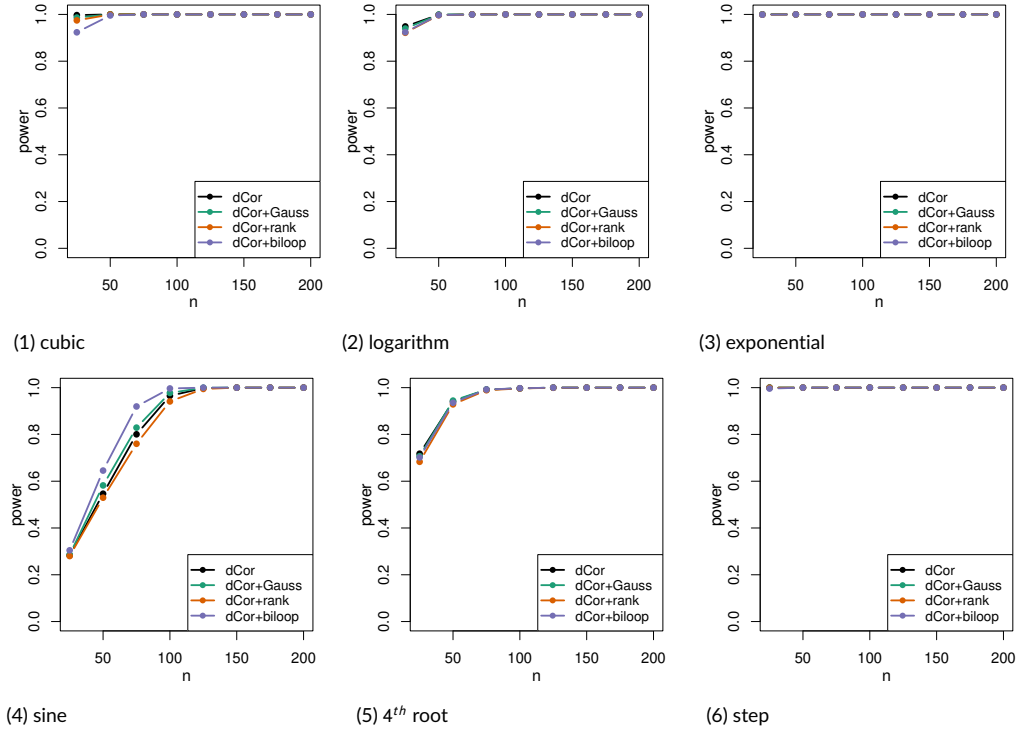


**FIGURE 24** Results of the power simulation per sample size  $n$ .

## F | MORE ON THE REAL DATA EXAMPLE OF SECTION 6

Among the genes for which the robust dCor with  $Y$  is below 0.05, the one with the second largest difference classical – robust has  $j = 5376$ , corresponding to gene U04636\_rna1\_at. Figure 25 is similar to Figure 20 in the main text, except that now five outliers are marked instead of four. The analysis is analogous.

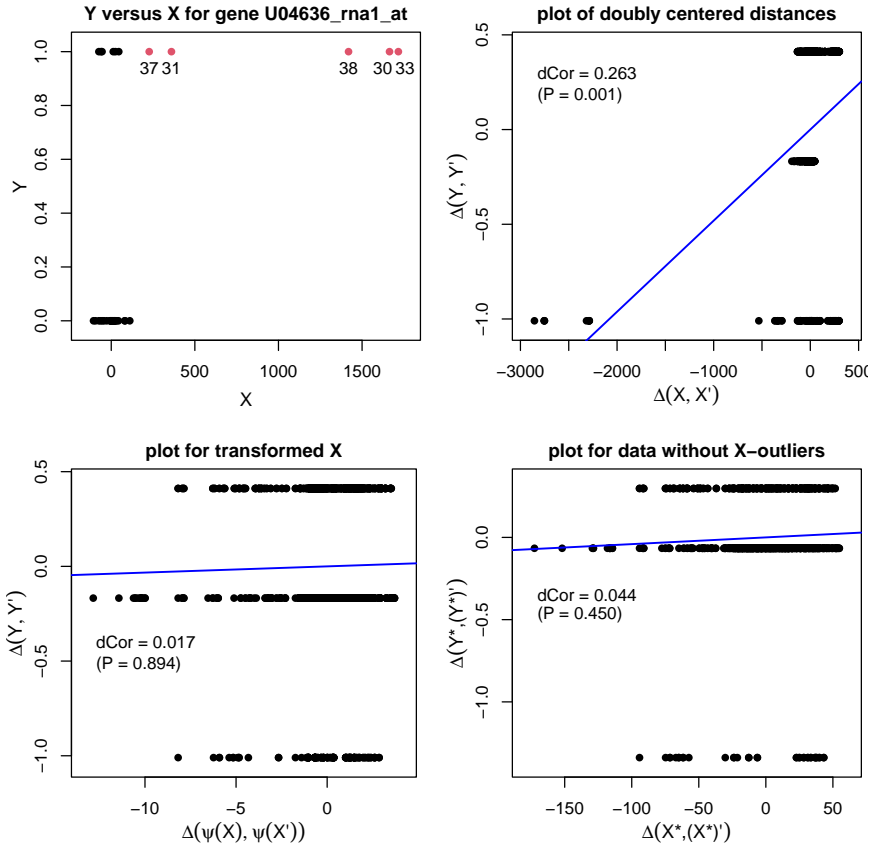


**FIGURE 25** Gene U04636\_rna1\_at of the leukemia data ( $j = 5376$ ). Top left: plot of  $Y$  versus  $X^j$ , with the five outliers marked in red. Top right: doubly centered distances  $\Delta(Y, Y')$  of  $Y$  versus those of  $X^j$ . Bottom left:  $\Delta(Y, Y')$  versus doubly centered distances of  $\psi_\infty(X^j)$ . Bottom right: plot of doubly centered distances for the data  $((X^j)^*, Y^*)$  without the five outlying points.

In the main text we analyzed gene Z19002\_at with  $j = 5071$ , where the robust dCor is higher than the classical one. In Figure 21 we saw that it has a single outlier in  $X^j$ , which does not obey the increasing trend of the remaining data points. Here we look instead at gene X57579\_s\_at ( $j = 5972$ ). Now the outlier (patient 38) has  $y_i = 1$ , which is in agreement with the increasing trend of the inliers. In a logistic regression, the fit would not change much because of this point. But here it still creates a far leverage point in the top right panel, which makes the Pearson correlation lower than when the point is removed, as seen in the bottom right panel. Another way to interpret this is that the

leverage point has reduced the slope of the regression line. Still, although the classical dCor is lower with the outlier than without it, here it remains significant in both situations.

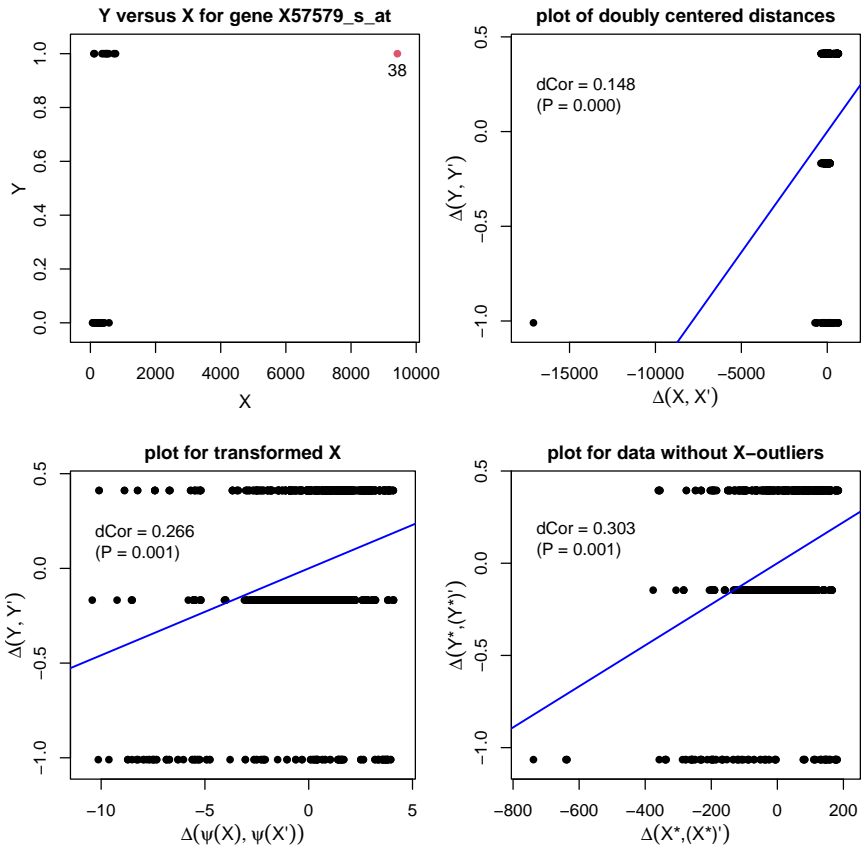


**FIGURE 26** The panels are as in Figure 25, but for gene X57579\_s\_at ( $j = 5972$ ).

## G | SUPPLEMENTARY MATERIAL FOR THE REJOINDER

In our reply to the invited comment by Klaus Nordhausen and Una Radojčić we gave a counterexample to the sub-additivity of  $d\text{Var}$  using Bernoulli distributions. Consider  $X \sim \text{Bernoulli}(p)$  with success probability  $0 < p < 1$  and  $X', X''$  independent copies of  $X$ . We used that

$$d\text{Var}(X) = \mathbb{E}[|X - X'|^2] + \mathbb{E}[|X - X''|^2] - 2\mathbb{E}[|X - X'| |X - X''|] = 4p^2(1-p)^2.$$

This is found as follows. We have that

$$d\text{Var}(X) = \mathbb{E}[|X - X'|^2] + \mathbb{E}[|X - X''|^2] - 2\mathbb{E}[|X - X'| |X - X''|].$$

Now  $\mathbb{E}[|X - X'|] = 2p(1-p)$ ,  $\mathbb{E}[|X - X'|^2] = 2p(1-p)$ , and  $\mathbb{E}[|X - X'| |X - X''|] = p(1-p)^2 + (1-p)p^2$  (note that  $|X - X'| |X - X''| \neq 0$  only if  $(X, X', X'') = (1, 0, 0)$  or  $(X, X', X'') = (0, 1, 1)$ , which happens with probabilities  $p(1-p)^2$  and  $(1-p)p^2$ ). So we have  $d\text{Var}(X) = 2p(1-p) + (2p(1-p))^2 - 2(p(1-p)^2 + (1-p)p^2) = 4p^2(1-p)^2$ .

Now consider  $Z := X + X'$ . Then

$$Z = \begin{cases} 0 & \text{with probability } P_0 := (1-p)^2 \\ 1 & \text{with probability } P_1 := 2p(1-p) \\ 2 & \text{with probability } P_2 := p^2. \end{cases}$$

As a result, we have

$$\begin{aligned} \mathbb{E}[|Z - Z'|] &= 2 * P(|Z - Z'| = 2) + P(|Z - Z'| = 1) \\ &= 2(2P_0P_2) + (2P_0P_1 + 2P_1P_2) \end{aligned}$$

and similarly

$$\begin{aligned} \mathbb{E}[|Z - Z'|^2] &= 4 * P(|Z - Z'| = 2) + P(|Z - Z'| = 1) \\ &= 4(2P_0P_2) + (2P_0P_1 + 2P_1P_2). \end{aligned}$$

The third term is the most cumbersome. The joint distribution of  $(Z, Z', Z'')$  is given by the following table:

$Z$	$Z'$	$Z''$	$ Z - Z'  \cdot  Z - Z'' $	Probability
0	0	0	0	$P_0^3$
0	0	1	0	$P_0^2 P_1$
0	0	2	0	$P_0^2 P_2$
0	1	0	0	$P_0 P_1 P_0$
0	2	0	0	$P_0 P_2 P_0$
1	0	1	0	$P_1 P_0 P_1$
1	1	0	0	$P_1^2 P_0$
1	1	1	0	$P_1^3$
1	1	2	0	$P_1^2 P_2$
1	2	1	0	$P_1 P_2 P_1$
2	0	2	0	$P_2 P_0 P_2$
2	1	2	0	$P_2 P_1 P_2$
2	2	0	0	$P_2^2 P_0$
2	2	1	0	$P_2^2 P_1$
2	2	2	0	$P_2^3$
0	1	1	1	$P_0 P_1^2$
1	0	0	1	$P_1 P_0^2$
1	0	2	1	$P_1 P_0 P_2$
1	2	0	1	$P_1 P_2 P_0$
1	2	2	1	$P_1 P_2^2$
2	1	1	1	$P_2 P_1^2$
0	1	2	2	$P_0 P_1 P_2$
0	2	1	2	$P_0 P_2 P_1$
2	0	1	2	$P_2 P_0 P_1$
2	1	0	2	$P_2 P_1 P_0$
0	2	2	4	$P_0 P_2^2$
2	0	0	4	$P_2 P_0^2$

Therefore we can calculate the probabilities of  $|Z - Z'| |Z - Z''|$  taking on the values 1, 2 and 4 by summing the corresponding probabilities in the table. We get

$$P(|Z - Z'| |Z - Z''| = 1) = P_0 P_1 (P_0 + P_1) + P_1 P_2 (2P_0 + P_1 + P_2) = P_1 P_0 (P_0 + P_1 + 2P_2) + P_1 P_2 (P_1 + P_2),$$

$$P(|Z - Z'| | |Z - Z''| = 2) = 4P_0P_1P_2,$$

$$P(|Z - Z'| | |Z - Z''| = 4) = P_0P_2(P_0 + P_2).$$

Combining these results yields

$$\begin{aligned} d\text{Var}(Z) &= 4(2P_0P_2) + (2P_0P_1 + 2P_1P_2) + (2(2P_0P_2) + (2P_0P_1 + 2P_1P_2))^2 \\ &\quad - 2(P_0P_1(P_0 + P_1) + P_1P_2(2P_0 + P_1 + P_2) + 8P_0P_1P_2 + 4P_0P_2(P_0 + P_2)) \\ &= 16\rho^2 - 80\rho^3 + 176\rho^4 - 208\rho^5 + 144\rho^6 - 64\rho^7 + 16\rho^8 \end{aligned}$$

so finally

$$d\text{Var}(X + X') = 16\rho^2 - 80\rho^3 + 176\rho^4 - 208\rho^5 + 144\rho^6 - 64\rho^7 + 16\rho^8.$$

The resulting figure can also be confirmed empirically by the following R code:

```
dvarbern = function(pgrid, n){
  out = matrix(NA, nrow = length(pgrid), ncol = 3)
  i = 0
  for (p in pgrid) {
    i = i+1
    out[i,1] = p
    set.seed(1)
    x = rbinom(n, 1, p)
    y = rbinom(n, 1, p)
    out[i,2] = dcov::dcov(x + y, x + y)
    out[i,3] = dcov::dcov(x, x) + dcov::dcov(y, y)
  }
  out
}

pgrid = seq(0.01, 0.99, by = 0.01)
out = dvarbern(pgrid, n = 1e6)
outmat = rbind(c(0,0,0),out,c(1,0,0))
plot(outmat[,c(1,3)], type="l", col="red", xlab="p",
      ylab = "dVar(X+Y) and dVar(X)+dVar(Y)")
lines(outmat[,c(1,2)], col="blue")
abline(h=0)
abline(h=0.5, lty = 2, lwd = 1)
```